Energy & Environmental Science

ROYAL SOCIETY OF CHEMISTRY

REVIEW

View Article Online
View Journal | View Issue

Cite this: *Energy Environ. Sci.*, 2021, **14**, 4203

The role of supercritical carbon dioxide for recovery of shale gas and sequestration in gas shale reservoirs†

Qiao Lyu, [a] Jingqiang Tan, *[a] Lei Li, [a] Yiwen Ju,*[b] Andreas Busch, [c] David A. Wood, [d] Pathegama Gamage Ranjith,[e] Richard Middleton,[f] Biao Shu,[a] Chenger Hu,[a] Zhanghu Wang[a] and Ruining Hu[a]

The development of hydraulic fracturing and horizontal drilling techniques has promoted the exploitation of shale gas resources. However, using water has several potential drawbacks including environmental issues, *e.g.*, the contamination of groundwater, surface water, and soil. Supercritical carbon dioxide (SC-CO_2), with its special physical properties, has shown potential to enhance shale gas recovery replacing water as the stimulation fluid. This review summarizes the current status of shale gas recovery, the potential role of SC-CO_2 as a working fluid for shale gas recovery, and CO_2 geological sequestration in shale reservoirs. SC-CO_2 has a better rock-breaking capability than water, which is useful when drilling through shale formations. SC-CO_2 fracturing creates rougher and more complex fracture networks than hydraulic fracturing, leading to higher permeabilities. Some of the injected CO_2 for shale gas recovery could also be safely sequestered in shale reservoirs, thereby lowering carbon emissions and accessing CO_2 tax credits. However, shale–CO_2 or shale–water/brine–CO_2 interactions during & after shale gas recovery and sequestration can affect reservoir properties. The implied shale–CO_2 imbibition process from available data generally persists for several years, far more than the several days assumed for most laboratory tests. A more detailed understanding is required for SC-CO_2 injection on the efficiency of shale gas recovery and the cost and environmental concerns of this technology. This will support the development of safe sequestration methods, supported by suitable laboratory and field tests, especially those focusing on geochemical, petrophysical, geomechanical and hydraulic properties.

Received 18th November 2020,
Accepted 16th April 2021

DOI: 10.1039/d0ee03648j

rsc.li/ees

Broader context

The production of shale gas has been drastically increased because of the development of hydraulic fracturing. Though shale gas is a much cleaner energy resource compared to coal and oil, hydraulic fracturing has potential environmental impacts, *e.g.*, the large consumption of water and the contamination of groundwater and earth surface. Supercritical carbon dioxide (SC-CO_2), with its special physical properties, has shown potential to enhance shale gas recovery replacing water as the stimulation fluid. This article summarizes the current status of shale gas development, the potential role of SC-CO_2 as a working fluid for shale gas recovery, and CO_2 geological sequestration in shale reservoirs. Meanwhile, the challenges of SC-CO_2 fracturing in shale reservoirs are discussed in detail. Particularly, the concerns of SC-CO_2 enhanced shale gas recovery are addressed which includes diffusion and adsorption of CO_2 in shale gas reservoirs, the CO_2–shale or CO_2–water–shale interactions and related changes in shale properties, and further concerns such as the costs, environmental impacts, and life cycle assessments of using SC-CO_2 for shale gas extraction. This review provides an overall understanding of the application of SC-CO_2 in shale gas development and the feasibility of CO_2 sequestration in shale reservoirs.

[a] *Key Laboratory of Metallogenic Prediction of Nonferrous Metals and Geological Environment Monitoring, School of Geosciences and Info-physics, Central South University, Changsha 410083, China. E-mail: tanjingqiang@csu.edu.cn*
[b] *Key Laboratory of Computational Geodynamics, College of Earth and Planetary Sciences, University of Chinese Academy of Sciences, Beijing, 100049, China. E-mail: juyw03@163.com*
[c] *The Lyell Centre, Institute of GeoEnergy Engineering, Heriot-Watt University, Edinburgh, EH14 4AS, UK*
[d] *DWA Energy Limited, Lincoln, LN5 9JP, UK*
[e] *Deep Earth Energy Lab, Department of Civil Engineering, Monash University, Melbourne, 3800, Australia*
[f] *Carbon Solutions LLC, NM, 87545, USA*

† Electronic supplementary information (ESI) available. See DOI: 10.1039/d0ee03648j

1 Introduction

The United States Energy Information Administration (EIA) world energy outlook (2019) predicted that world energy demand will rise nearly 50% between 2018 and 2050, and fossil fuel will still be the dominant energy source.[1] As stated in the 2015 Paris Agreement as well as the Intergovernmental Panel on Climate Change (IPCC), the transition to consuming more environmentally friendly energy is being pursued as a matter of

urgency by many counties to meet the 1.5 °C target.[2] Compared to oil and coal, natural gas is a much cleaner energy source, producing only 45% of the carbon dioxide (CO_2) of coal.[3] Unconventional gas (*e.g.* shale gas or tight gas), which is known to be present in large resource quantities around the world, shows potential as a bridging fuel to transition to renewable energy sources. Natural gas from shale could adequately supply the continued growth in energy demand for developing economies in the next few decades and contribute significantly to the demand for decreasing CO_2 emissions.[4]

The development of hydraulic fracturing and horizontal drilling techniques has promoted the rapid exploitation of shale gas resources, particularly in North America.[3,5] In the US, shale gas production increased from 1990 billion cubic feet in 2007 to 23 550 billion cubic feet in 2018.[6] In addition to the US and Canada, other countries like China and Argentina are making progress in commercial shale gas production. However, drilling, and hydraulic fracturing require large amounts of water. In the US, the amount of injected water per well is 10 000 to 50 000 cubic meters, only 9–34% of which returns to the surface after hydraulic fracturing.[7–11]

Based on the research from the World Resources Institute (WRI), eight of the top 20 countries with the largest shale gas resources face arid conditions or high to extremely high baseline water stress where the shale resources are located. China and India, which account for one-third of the world's population, are included in the eight countries. The widespread use of hydraulic fracturing will put more people at risk of water shortages and more pressure on existing water resources.[12]

The fracturing fluids are usually composed of water plus proppant ($\geq 98\%$) and chemical additives ($< 2\%$).[13] It has been estimated that about 14 types of chemicals are used in each well, such as gelling agents to improve the carrying ability of proppant, hydrochloric acid to open the fractures and dissolve carbonate minerals, friction reducers (slick water) to aid the penetration of the injected fluids and other substances.[14–16] Some chemical additives are toxic and some toxic substances are produced during fracturing,[13] although, over time, the toxic components historically used in fracturing fluids have been significantly reduced by most operators under pressure to reduce their environmental impacts. The residual fracturing fluids in the shale reservoirs and the disposal of flowback water potentially leads to the contamination of groundwater, surface water, and soil if not handled carefully.[17–20] In addition, hydraulic fracturing can induce microseismic events.[21] Based on the above drawbacks, Western Australia, New Brunswick, and California, as well as France, Ireland, and South Africa have banned hydraulic fracturing. Therefore, it is essential to explore new approaches for shale gas recovery which could reduce or even eliminate water consumption in fracture stimulation.[22,23]

With its attractive physical properties (*e.g.*, liquid-like density, gas-like viscosity, no capillary force and good miscibility with hydrocarbons), supercritical carbon dioxide (SC-CO_2) is now under consideration as a fracture stimulation fluid or component of energized fluids injected into unconventional shale or tight gas reservoirs to enhance gas recovery.[24–27] Similar to slick water, the low viscosity of SC-CO_2 can create complex, multi-orthogonal fracture networks allowing high flow rates.[28] SC-CO_2 has a lower value of chemical potential than methane,[29] which offers a significant advantage over water in that methane can be easily desorbed by SC-CO_2 as the adsorptive capacity of SC-CO_2 in shale is about 2–3 times higher than methane.[30] In addition, shale gas reservoirs have the potential to become targets for CO_2 sequestration when using SC-CO_2 as the fracturing fluid,[31–33] The development of techniques for capturing CO_2 from fossil-based power plants and the atmosphere will make it possible to offer sufficient CO_2 for shale gas recovery.[34–36] Meanwhile, obstacles like the current high costs of capturing, pressurizing, and transporting of CO_2, the efficiency of shale gas recovery affected by CO_2–shale interactions, and the reliability of long-term entrapment and safety of CO_2 sequestration in shale reservoirs, remain uncertain. The IPCC report states that CO_2 emission reduction targets can only be met if carbon capture and storage significantly contribute to the mitigation strategies. If implemented, CO_2 will become available in significant amount, ultimately reducing costs for capturing.

This paper systematically summarizes the current status of shale gas exploitation, the geological utilization and sequestration of CO_2, and the role of SC-CO_2 in shale gas recovery including SC-CO_2 used as a drilling fluid, SC-CO_2-based fracturing, and CO_2 storage in shale gas reservoirs. The advantages and drawbacks of these (SC-)CO_2-related studies and applications in literature are discussed. Further, the concerns of SC-CO_2 enhanced shale gas recovery are addressed which includes diffusion and adsorption of CO_2 in shale gas reservoirs, the CO_2–shale or CO_2–water–shale interactions and related changes in shale properties, and further concerns such as the costs and the environmental impacts of SC-CO_2 injection for shale gas recovery. Challenges and perspectives are presented to expand our understanding and verify the feasibility of SC-CO_2 enhanced shale gas recovery and CO_2 sequestration in shale gas reservoirs.

2 Shale gas and exploitation

2.1 Global shale gas resources and exploitation status

Based on the EIA findings in 2016, the world's technically recoverable shale gas resources are over 200 trillion cubic meters (TCM), which could support global natural gas consumption for more than six decades based on current gas consumption.[37] Fig. 1 shows the distribution of the global shale gas resources: China has the largest gas reserves of 36.1 TCM. However, in 2019, China's foreign dependence on oil and natural gas amounted to 72% and 43%, respectively.[38] The US and Argentina have the second and third highest resources with 24.4 and 21.9 TCM, respectively. However, it should be noted that many countries and regions have yet to fully evaluate and quantify their shale gas resources; especially in the Middle East, Australia, North Africa, and Russia where large resources are expected. Though such evaluations could change over time as more data

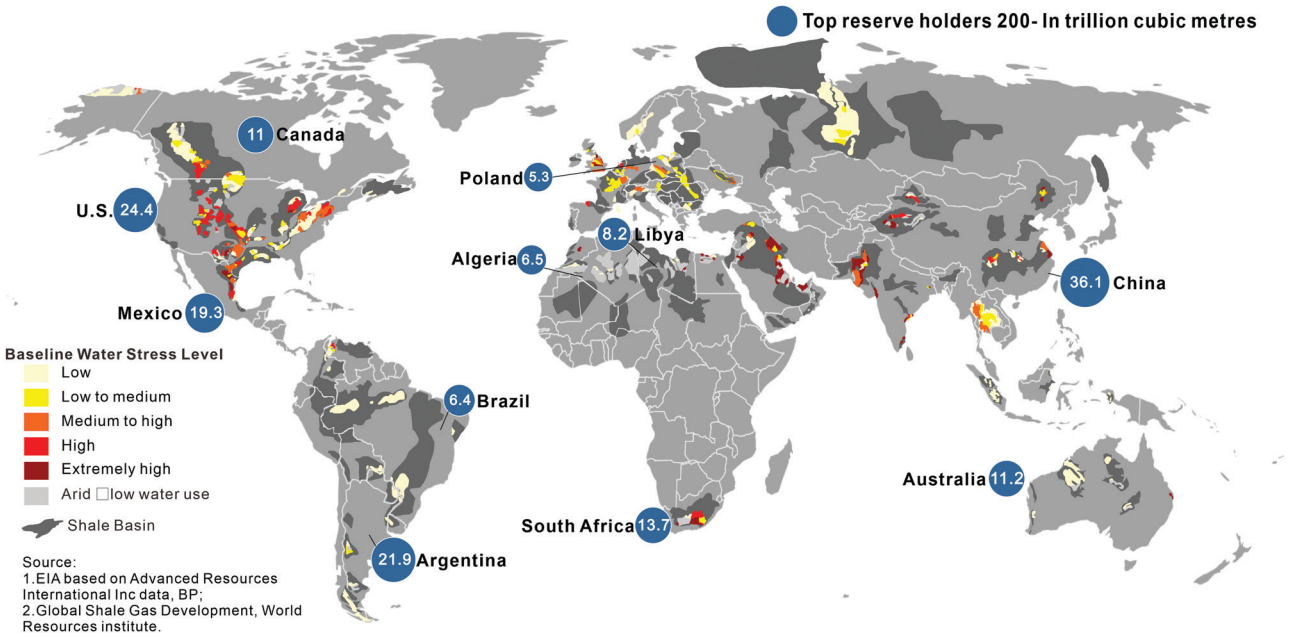

Fig. 1 The global shale gas resources.[12,39]

becomes available, the reserves of unconventional natural gas, *e.g.*, shale gas, are widely considered to be significantly greater than conventional natural gas.

North America was the first region of the world to achieve commercial shale gas production. From 2007 to 2018, shale gas production increased by 702% to 0.6072 TCM per year,[40] which is expected to increase until 2050. Texas' Barnett shale was the first formation to commercially produce large quantities of shale gas and was the beginning or rapid technology development.[41] The large-scale recovery of shale gas has helped the US to transform from an importer of natural gas into an exporter.[3,42] Shale gas recovery has also rapidly developed in Canada. Although hydraulic fracturing is suspended or prohibited in the east of the country, shale gas production is expected to grow to annual values of 0.1926 TCM in 2050, mainly from western Canada.[43] Commercial shale gas production in China commenced in 2010 and has grown continuously reaching annual volumes of 0.0154 TCM in 2019, making it the world's second-largest shale gas producer.

2.2 Overview of current gas recovery methods and fracturing fluids

Unconventional tight reservoirs, such as shale oil/gas, tight gas or coalbed methane, are characterized by their low permeability which is typically <1 mD.[44,45] Therefore, advanced technologies such as horizontal drilling and multi-stage fracturing are required to commercially recover gas from such reservoirs.[46–49]

Shale formations are often characterized by laminated morphologies made up of multiple thin layers. Regionally, in broad basins the formations tend to be dominated by shallow dips, particularly in the deeply buried, thermally mature basin centers. In such conditions, horizontal wells can access much larger volumes of shale gas than vertical wells.[50] When the vertical well reaches the shale formation, the drilling trajectories are adjusted by nearly 90 degree to a near-horizontal direction. One vertical well is likely to be branched into several lateral horizontal wells extending into the shale formation in different directions, like a radial net. The length of the horizontal well is commonly about 1 to 2 km.[51] Horizontal drilling cannot on its own offer sufficient flow paths for gas moving from the adjacent shale formations into the wellbores. Therefore, hydraulic fracturing is needed to extract shale gas economically. Hydraulic fracturing is now widely used to enhance the production of unconventional oil and gas which are stored in tight reservoirs. During a hydraulic fracturing operation, high-pressure water is injected into a well and flows through the perforated zones. Fractures are created around and beyond the well. The hydraulic conductivity increases substantially following fracture stimulation, allowing more gas to be drained and flow into the wellbore.[52] In order to maximize the fracturing efficiency, multi-stage hydraulic fracturing has become the standard stimulation technique applied to horizontal wellbores.[53,54]

There are various types of fracturing fluids employed for unconventional oil and gas recovery, which can be categorized as liquid-based fluids, foam-based fluids, and gas-based fluids, as shown in Table 1.

Water-based fluids were first used for hydraulic fracturing in Kansas in 1947.[63] Slickwater, which is comprised of water-based fluids by 90 vol%, has the benefit of producing multi-fracture networks with high penetration depths, resulting in significantly enhanced permeabilities. Although such fluids are commonly the first choice for developing shale gas reservoirs, they have substantial drawbacks in certain locations and formations. Injecting large amounts of water typically results in a range of water–rock interactions, potentially causing formation damage.[64]

Table 1 The typical fracturing fluids used to stimulate tight gas and oil reservoirs

Liquid-based[55–57]	Foam-based[58–60]	Gas-based[61,62]
Water-based fluids	Acid-based foams	Air
Acid-based fluids	Liquid CO_2-based foams	CO_2
Alcohol-based fluids	Hydrocarbon-based foams	N_2
Emulsion-based fluid	Alcohol-based foams	
Liquefied petroleum gas (LPG) fluids		

Mineral precipitation like carbonates can cause fracture closure and plugging of pore throats, thereby either decreasing fracture and/or matrix permeability or fully preventing accessibility to certain parts of the reservoir. The disposal of these vast amounts of back-produced fracturing fluids and formation waters requires huge capital expenses and, in some locations, the risk of impacting drinking water resources through aquifer contamination is given.[65] To improve gas recovery from tight reservoirs, chemical additives are used in hydraulic fracturing fluids, which are increasingly recycled after back-production for reuse in subsequent stimulations. For example, polymer viscosifying agents are added in slickwater to improve its proppant-carrying ability. Hydrochloric or muriatic acid improves mineral dissolution which helps to enlarge fractures. However, some of these additives will produce toxic substances which, if not treated carefully, can lead to environmental contamination issues both above and below ground.[20,66,67] Due to these issues and concerns about long-term effects associated with potential negative environmental impacts, the wide use of water-based fracturing fluids is contentious and a substantial number of countries and regions have enacted legislation to prohibit the use of hydraulic fracturing, at least temporarily while studies are conducted to better understand its impacts, and methods and materials are developed to mitigate its downside risks.[68]

The application of foam as a fracturing fluid has been investigated since the 1970s.[69] Compared to water-based fluids, foam-based fluids present several desirable properties as potential fracturing fluids. Foams mainly consist of gas (60 to ~95%, depending on the foam quality), reducing the consumption of water considerably. Foam has a high proppant-carrying and proppant-suspending capability, quick fluid recovery, low fluid loss into the formation and generally shows low formation damage.[70,71] CO_2 and N_2 based foams are used most widely to replace water-based fracturing fluids.[72] Compared to CO_2 based foams, N_2 based foams are generated at a low hydrostatic pressure, so that high surface pumping is necessary for most field applications, making this a relatively energy-intensive approach.[58] On the other hand, CO_2 transitions to its supercritical state when pumped into shale reservoirs.[73] The behavior of SC-CO_2 foam-based fluids is complicated because the multiphase flow includes a supercritical phase.[74] To maintain the stability of fracturing fluids at high temperatures and pressures in shale reservoirs, surfactants and other chemicals are added during the process of foam generation at the surface.[75] As with water-based fracturing fluids, the potential environmental impacts of these additives raise concerns about foam-based fracture stimulation fluid applications on a large scale.

Among the gas-based fracturing fluids, N_2 has received more attention in research studies.[76–80] Fracturing with N_2-based foams consumes relatively little water and low quantities of chemical additives. Despite the easy accessibility, the large consumption of N_2 in the stimulation of each well makes the fracturing process expensive. The low viscosity of N_2 further limits its proppant suspension and transportation capability. N_2-based fracturing can also induce self-propping fractures which contribute to fracture opening.[81] However, this phenomenon is typically only induced on a meaningful scale in shallow wells. For shale reservoirs in China for example, most of which are deeper than 3000 m, self-propping typically only makes a minor contribution.

2.3 Drawbacks of hydraulic fracturing

2.3.1 Environmental concerns. In general, environmental concerns associated with unconventional oil and gas development can be categorized into four main groups, including community issues (*e.g.*, industrial noise and induced seismicity), water issues (*e.g.*, groundwater and surface water contamination), land issues (*e.g.*, ecosystem impacts), and atmospheric issues (*e.g.*, air pollution).[82–84] Recently, there is extensive research and debate in academia, industry, and society in general about the environmental impacts of unconventional reservoir development. In 2016, the US Environmental Protection Agency (EPA) reported the impacts of hydraulic fracturing water cycle on drinking water resources.[85] It is widely recognized that the injection of water at high-pressure into subsurface formations can lead to pollution of the hydrosphere, biosphere, and atmosphere with serious consequences for flora and fauna and the quality of drinking waters. Another consequence is induced seismicity which may cause damage to surface structures, associated risks of personal injury, and potentially compromise the integrity of wellbores and other subsurface infrastructure (*e.g.*, flowlines and pipelines).[7,84,86–90] Among all above mentioned environmental risks, water issues, including water use and reuse, water contamination, and wastewater disposal, are the most direct and perhaps have the greatest negative impacts.

The hydraulic fracturing fluid generally consists of three components:[91] (i) the base fluid, which is the largest constituent (usually 98% or more) by volume and is typically water, (ii) the additives, which are generally a mixture of chemicals (as listed in Table 2), and (iii) the proppant, which is solid material designed to keep hydraulic fractures open. The chemical additives in the fracturing fluid and the products of their interaction with the organic matter and radioactive elements in the formation are initially released into the subsurface shale formation, some of which eventually flows back to the surface.[92] The flow-back water may contaminate underground drinking water sources and the surface environment if not carefully handled.[93,94] Of course, there has been a continuous effort to develop safer additives, and more

Table 2 Common chemical additives in hydraulic fracturing fluids[92]

Additive type	Example compounds	Purpose
Acid	Hydrochloric acid	Wellbore clean out, mineral dissolution, fracture initiation
Friction reducer	Polyacrylamide, petroleum distillate	Minimize friction between fracturing fluid and wellbore pipe
Corrosion inhibitor	Isopropanol acetaldehyde	Pipe corrosion prevention by diluted acid
Iron (Fe^{2+}) control	Citric acid, thioglycolic acid	Prevent precipitation of metal oxides
Biocide	Glutaraldehyde, 2,2-dibromo-3-nitrilopropionamide (DBNPA)	Bacterial control
Gelling agent	Guar/xantham gum or hydroxyethyl cellulose	Thicken water to suspend proppants (*e.g.* sand)
Crosslinker	Borate salts	Maximize fluid viscosity at high temperatures
Breaker	Ammonium persulfate, magnesium peroxide	Promote breakdown of gel polymers
Oxygen scavenger	Ammonium bisulfite	Remove oxygen from fluid to reduce pipe corrosion
pH adjustment	Potassium or sodium hydroxide or carbonate	Maintain effectiveness of other compounds (such as crosslinker)
Proppant	Silica quartz sand	Keep fractures open
Scale inhibitor	Ethylene glycol	Reduce deposition on pipes
Surfactant	Ethanol, isopropyl alcohol,2-butoxyethanol	Decrease surface tension to allow water recovery

importantly, there are no documented cases of propagation and contamination of fracturing fluid to shallow aquifers, though the potential for hydraulic fractures to propagate to the near-surface deserves special concern.[85] Water contamination may occur especially in scenarios of shallow fracturing in the vicinity to aquifers and/or the regional groundwater levels, poorly cemented casing in the wellbores, and surface spills due to equipment failures or improper fluid-handling operations.[66,95,96] In addition to the leakage of fracturing fluids, flow-back fluids and wastewater may perturbate the groundwater equilibrium and the stability of geochemical and hydrodynamic processes in the subsurface.[88]

The development of shale gas plays can also lead to air pollution. Greenhouse gases, such as methane from fugitive emissions and carbon dioxide, and toxic gases like ozone and aromatic-rich vapors released from aromatic hydrocarbon liquids such as benzene, are produced regularly during fracture stimulation activities. The released greenhouse gases can degrade air quality and contribute to climate change. The toxic components can have negative health impacts and cause eco-system damage.[97,98]

2.3.2 Poor hydrocarbon recovery. Shale is mostly water-wet and the initial water saturation is less than 100%.[99,100] During the shale gas recovery process *via* hydraulic fracturing, water will imbibe into microfractures and shale pore system. Because of the capillary force, water will stay in the fractures or pores which narrows or even block the gas flow pathways.[101] Therefore, the permeability of shale will decrease after water imbibition.[102–104] The reduction of shale permeability will increase with the increase of water saturation.[47,105]

Injecting large amounts of water into shale reservoirs may cause specific water–shale interactions, potentially leading to reduced hydrocarbon recovery. Swelling clays, such as smectite, have the ability to take up water, leading to a volumetric expansion. If present in the shale reservoir, this can result in a reduction in pore and pore throat sizes.[106] The swelling potential can be classified by the activity value which is a ratio of plasticity index and clay fraction.[107] Fig. 2 summarizes the swelling potential of several shales with different clay fractions.[108–111] It can be seen that shales present appreciable swelling potential which increases with increased clay content. Even with clay content as low as 7%,[112] the maximum free swelling percentage was about 1.6%. The swelling of shale can

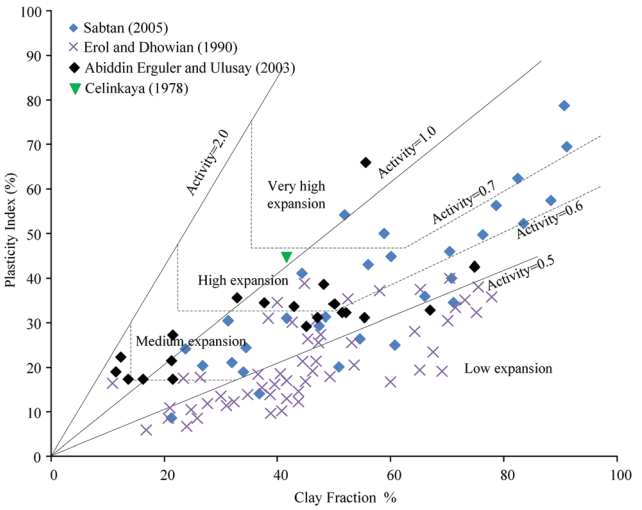

Fig. 2 The swelling potential of shale with different clay fractions.[108–111]

decrease the accessible specific surface area, ultimately reducing gas that could desorb and produced from the shale matrix.[113] As water filtrates into cracks and pores, it tends to block the pore throats and trap hydrocarbons. The water-blocking effect leads to a decrease in permeability.[102,114]

3 CO_2 emissions and CO_2 utilization, and storage

3.1 Anthropogenic CO_2 emissions and global impacts

Present and future worldwide economic growth relies on the consumption of fossil fuels. Coal, oil and natural gas are responsible for a large amount of the global energy supply and similarly contribute to overall CO_2 emission.[115] In 2019, a total of 33.3 gigatons (Gt) of CO_2 were emitted to the atmosphere globally, which is ~60% higher than in 1990.[116] In the US, more than 60% of the total stationary CO_2 emissions are contributed by large stationary sources, like power plants, cement production plants, iron and steel manufacturing facilities, *etc.*[117] It is important to note that different stationary sources have different CO_2 quantities in their flue gases. Coal

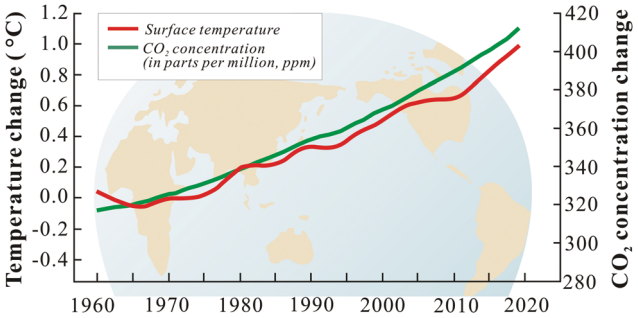

Fig. 3 The variations of CO_2 concentration/earth temperature with years.[122,123]

and natural gas-fired power plants, which are the major sources of CO_2 with large flow rates, have flue gas compositions containing only 4–14% CO_2. On the other hand, flue gas CO_2 compositions of iron and steel production, agricultural processing and sugar production plants are often higher than 40%. The IPCC emphasizes that a 50% reductions of CO_2 emission should be reached to limit the rise of global average temperature to 2–2.4 °C by 2050.[118,119] How to limit the growth of CO_2 emission has become a worldwide challenge and technically feasible and cost-effective solutions are not yet readily available.

In line with increasing CO_2 emissions, atmospheric CO_2 concentration have increased drastically at the same pace with the Earth's temperature (Fig. 3). This increasing trend is expected to continue due to forecasted global economic growth and industrial development.[120] Consequently, global warming is generally expected to increasingly result in climate change which has significant impacts on all ecosystems.[121] Consequently, CO_2 emissions need to be limited to protect the environment for the benefit of all life on Earth.

3.2 CO_2 utilization and sequestration in geoenergy exploitation

CO_2 capture, utilization, and storage (CCUS) is considered a key requirement to limit CO_2 emissions to the atmosphere, contributing at least one-sixth of global CO_2 emission reductions by 2050.[124] It is further estimated that CCUS will lead to a 14% reduction in cumulative emissions between 2015 and 2050 to achieve the targeted 2 °C scenario by 2050, and thereby reduce the overall costs required to mitigate the negative global impacts of climate change.[124] The utilization and sequestration of CO_2 in energy exploitation have shown promising potential to decrease the total CO_2 emission.

3.2.1 CO_2 utilization. The utilization of CO_2 can be divided into two types: physical utilization and chemical utilization.[119] The physical utilization means CO_2 is directly used without any conversion,[125] while the chemical utilization involves CO_2 being partially or totally converted to chemicals and fuels.[126–128] Norhasyima and Mahlia[129] have statistically analyzed the CO_2 utilization methods from 3002 related patents searched from the Derwent Innovation. They found that, more than half of them were related to chemicals and fuel, a quarter d to enhanced oil (EOR) and enhanced coalbed methane (ECBM) recovery, 16.3% to biofuels from microalgae, mineral carbonation accounted for 3.4% and enhanced geothermal system (EGS) contributed 1.5%. The patent applications provide insight to the potential utilization of CO_2 in geoenergy recovery.

3.2.1.1 CO_2-EOR. The primary oil recovery for conventional and unconventional formation is less than 20% and 10%, respectively.[130,131] This means that large quantities of oil remain in the reservoir. The injection of CO_2 has the potential to increase oil recovery by 5–15%.[132–134] A schematic diagram for CO_2 enhanced oil recovery is shown in Fig. 4. The potential additional oil recovery by secondary and tertiary recovery using carbonated (or CO_2-saturated) water injection is 6.2–56.74% and 9–40.54%, respectively.[135] The injection of CO_2 increases the pressure of depleted oil formations and decreases the viscosity of oil, thereby creating high flow rates and mobility for additional recovery of oil. Meanwhile, CO_2 especially under supercritical conditions, is a highly effective solvent that can decrease the viscosity of oil, allowing the oil to flow through the reservoir and into wellbores more easily.[136–138] CO_2 can penetrate into micropores and nanopores and dissolve the oil, leading to oil expansion. The increase in oil volume makes the oil easier to migrate in the reservoir and to the production well. Intermediate components of oil gradually form the miscible phase with CO_2, reducing the oil and gas interfacial tension.[139–141] Because of these benefits, CO_2-EOR has been applied in many countries. As of 2019, there are more than 150 individual CO_2-EOR projects around the world.[142]

3.2.1.2 CO_2-ECBM. In 2017, the proven coalbed methane reserves in the US were 11 TCF,[144] with a recovery efficiency of 20–60%.[145] Coalbed methane can be enhanced by CO_2 injection as a secondary recovery mechanism.[146,147] The injection of CO_2 maintains the pressure of the coal seams and higher sorption ability promotes methane desorption from internal porous surfaces of coal. Then the desorbed methane migrates through the pore space or cleats (fractures in coal) to the production well.[145,148–151] Several pilot and micro-pilot projects of CO_2-ECBM have been applied in Australia, Canada, Japan, China, Poland and the US.[150]

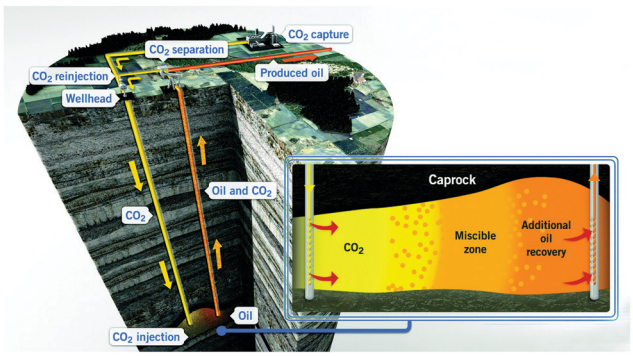

Fig. 4 A schematic diagram for CO_2-EOR.[143]

3.2.1.3 Other utilization methods. (1) Chemicals and fuel. In the chemical industry, CO_2 is a suitable feedstock in fuel cells or hydrogen sources for electricity.[152,153] CO_2 can also be used to manufacture urea, salicylic acid, cyclic carbonates, formic acid and polycarbonates.[154] However, current market demands for these products are relatively small. (2) Mineral carbonation. Some carbonates such as magnesium carbonate ($MgCO_3$) and calcium carbonate ($CaCO_3$), can be produced through CO_2 mineralization processes.[155] Feedstocks like natural silicate ores[156] and alkaline solid wastes[157,158] can be used in these processes. The mineralization is achieved by four methods: direct and indirect carbonation, carbonation curing, and electrochemical mineralization.[159,160] (3) Enhanced geothermal systems (EGS). A typical EGS uses water or brine as the heat exchange fluid. Recent studies have shown that CO_2 could be an alternative working fluid because of the following advantages: a poor solvent for the minerals, low viscosity which leads to high heat extraction rate, and large compressibility and expansibility which can generate favorable buoyancy forces.[161–165] (4) Biological algae cultivation. Algae are among the oldest phototrophic organisms to evolve on Earth and they have the ability to utilize CO_2 as a food source from the atmosphere, soluble carbonates, and discharged gases from heavy industry. Algae cultivation can be performed in an open or closed systems and controlled by various precursors.[166] Certain algae offer the potential to efficiently manufacture biodiesel on a commercial scale.[167]

3.2.2 CO_2 sequestration. Generally, the approach adopted for CO_2 sequestration is to capture CO_2 emission point sources like coal fired power plants, to transport it to an injection site, and to then sequester it in subsurface formation over long periods of time.[168,169] Considerable amounts of carbon dioxide will dissolve in formation waters, and might become mineralized (in the form of carbonates) over extended periods of time.[170,171] Potential CO_2 sequestration sites available are saline aquifers, depleted gas and oil reservoirs, unminable coal seams, and actively producing oil fields combined with enhanced recovery processes (see above).[172–177]

With more than 100 years of oil and gas exploitation, many oil and gas fields have already been depleted or are approaching the end of their commercially productive lives.[133] Benefits of CO_2 storage in depleted gas and oil reservoirs include:[178] (1) the oil and/or gas already removed offers plenty of original CO_2 storage capacity; (2) CO_2 can be stored at pressures that are close to the original reservoir pressure prior to production which avoids the risk of long-term formation damage and potentially inducing man-made subsidence at the surface; (3) the favorable geological conditions that originally facilitated oil and gas entrapment decrease the risk of CO_2 leakage through the primary caprock; (4) exiting wells and other infrastructure installed originally for oil and gas production purposes can be re-used for CO_2 injection. Meanwhile, the depths of most hydrocarbon fields are greater than 800 m, which ensures that the CO_2 would be stored in the supercritical phase.[179]

CO_2 sequestration projects have been applied by many countries, as listed in the ESI.† By October 2019, there were

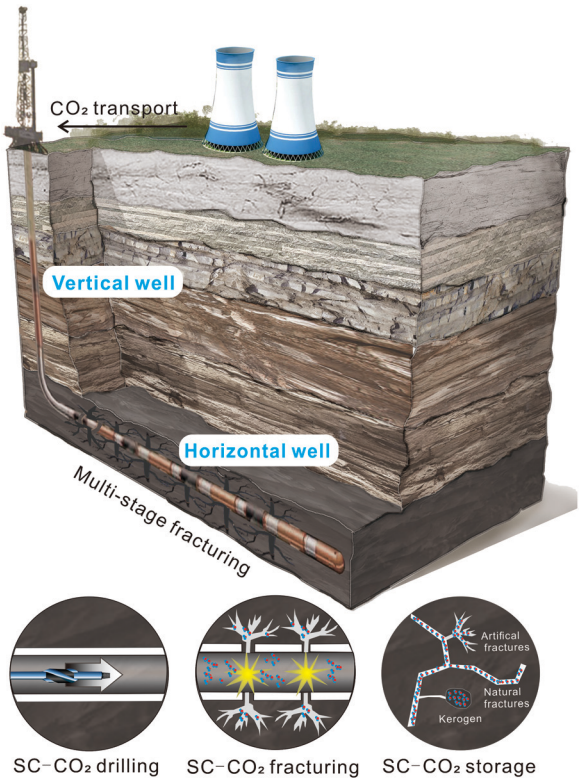

Fig. 5 The role of SC-CO_2 in shale gas recovery.

19 large-scale CCUS projects operating around the world storing ~32 Mt of CO_2 per year.‡[180] In the past 40 years, more than 1 billion tons of CO_2 were injected for CO_2-EOR operations in the US, and more than 99% of the injected CO_2 remains safely trapped.[181] The development of CO_2 geological storage still needs supports from the government, such as the 45Q tax incentive in the US,[182] and tools to better characterize and understand large-scale sequestration.[183,184]

4 Role of SC-CO_2 in shale gas recovery and sequestration in shale gas reservoirs

When studying shale gas recovery, SC-CO_2 has the potential to support three different key aspects: drilling, fracturing and long-term storage (Fig. 5). In this section, the potential of the three aspects are discussed.

4.1 SC-CO_2 based drilling

The high-pressure water-jet technology has been widely used for drilling in the oil and gas industry since the 1950s. To further improve the drilling efficiency and rock cutting or breaking performance, structures and properties of the water jet have been optimized to develop various types of jets (*e.g.*

‡ Large-scale projects are defined as those integrated projects that store at least 80 000 tons of CO_2 per year from a coal-based facility or at least 400 000 tons of CO_2 per year from other sources.

Table 3 Key findings of SC-CO_2 jet for drilling[195,198,199,201]

Effects	Key findings
Pressurization effect[195]	The pressurization effect during SC-CO_2 jet fracturing improves with an increase in pressure difference, ambient pressure, nozzle diameter, and fluid temperature; SC-CO_2 jet fracturing achieves improved pressurization compared to a water jet in deep boreholes.
Real gas effect[198]	Simulations covering the typical operating ranges (the liquid and supercritical regions) show that the Joule–Thompson throttling effects are much more prominent at higher inlet temperature and larger pressure drops.
Self-excited oscillation effect[199]	The impinging peak pressure is higher than that of the continuous SC-CO_2 jet; the frequency distribution is different from that of the self-excited oscillation pulsed water jet.
Stagnation effect[201]	The increase of injection pressure presents a large increase of the stagnation pressure and a minor decrease of the ambient temperature; the stagnation temperature is mainly controlled by injection temperature.

Table 4 The comparison of drilling ability between water and SC-CO_2[189,191–193,202]

Factor	Comparison between water and SC-CO_2
Threshold erosion pressure	SC-CO_2 is 56% lower than water (same condition in the Mancos shale)[189]
Specific cutting energy	SC-CO_2 is 97% lower than water (same condition in the Mancos shale)[189]
Cuttings transport ratio	SC-CO_2 is better than water because SC-CO_2 can maintain underbalanced conditions[191]
Erosion rate	SC-CO_2 is higher than water[192]
Rock-breaking depth	SC-CO_2 is deeper than water[193]
Cutting-carry ability	Water is better than SC-CO_2[202]

abrasive, cavitating, rotary, pulsed non-circular nozzle).[185–187] With the rapid development of deep resource exploration, more and more deep and ultra-deep vertical wells and long horizontal wells being used. This has intensified the demand for improving the rates of penetration (ROP) and minimizing the turn radius to reduce the cost of exploration and exploitation. The traditional high-pressure water jet offers few advantages for improving drilling efficiency because of the water-lock effect, the high threshold pressure for water jet erosion and the large pressure loss of coiled tubing.[188,189] Air drilling fluids like foams and nitrogen can create satisfactory underbalanced drilling (UBD) conditions which in many subsurface conditions are beneficial for the improvement of ROP. However, their low density makes it difficult for such fluids to provide sufficient torque for bottom hole motors to operate efficiently.[190] SC-CO_2, which has liquid-like density, is an attractive choice by the drilling industry for certain sub-surface conditions. Above critical temperature and pressure for CO_2, which is typically the case in shale gas reservoirs with horizontal wells, CO_2 is in the supercritical phase.

Kolle[189] was the first to conduct laboratory tests to evaluate the SC-CO_2 based drilling potential. The results show that the threshold erosion pressure for CO_2 is ~67% of water in the Sierra white granite and 44% of water in the Mancos shale. The specific energy for cutting granite with SC-CO_2 is 42% of water and only 3% of water in shale. Since then, other studies have used additional experimental and numerical methods to further investigate the SC-CO_2 jet. Gupta[191] developed a circulation model to calculate the SC-CO_2 jet impact force and the cuttings transport ratio. Results show the advantage of SC-CO_2 drilling, specifically that its liquid-like density can turn the downhole motor and gas-like viscosity can maintain underbalanced conditions. Al-Adwani, *et al.*[192] simulated the erosion rate of pure SC-CO_2 in UBD operations, concluding that SC-CO_2 is a viable UBD fluid.

In an experimental study using artificial rock cores, Du, *et al.*[193] found that a SC-CO_2 jet is able to achieve a higher rock-breaking depth than a water jet at the same pressure. Following these initial findings, a series of experimental and numerical studies were conducted to optimize the structure of nozzles which can improve the drilling ability of SC-CO_2 jets.[190,194–196] Meanwhile, further investigations were performed to analyze the flow field of SC-CO_2 jets in wellbore conditions.[197] It was found that the effects of pressurization,[198] real gas behavior,[199] and self-excited oscillations[200] in SC-CO_2 jets are beneficial for rock-breaking, while the stagnation effect[201] has a detrimental impact on drilling (Table 3). Considering the low viscosity, the feasibility of SC-CO_2 for carrying cuttings was experimentally and theoretically verified.[202] The results showed that cuttings are difficult to transport when the well angle is between about 60° and 80°. Fortunately, the viscosity of SC-CO_2 can easily be increased by adding additives such as the fluoroether disulfate telechelic ionomer, to improve its ability to effectively carry cuttings.[203] A comparison of drilling ability between water and SC-CO_2 is listed in Table 4.

4.2 Using SC-CO_2 as a fracturing fluid

SC-CO_2 fracturing has been investigated through experimental and numerical methods.[204–207] Due to its low viscosity and lack of surface tension, SC-CO_2 used as a fracture stimulation fluid, has the potential to lower the formation breakdown pressure and create more irregular multiple fractures compared to liquid CO_2 or water. Wang, *et al.*[208] used the Niobrara shale to conduct fracturing experiments with gaseous and SC-CO_2, as well as slickwater with the same confining pressures and temperature. They found that gaseous and SC-CO_2 induced fracturing occurred at much lower pressures than slickwater fracturing, which were 6.6 MPa, 9.6 MPa and 11.0 MPa, respectively. In a numerical study, investigating the fracturing process with water, viscous oil and SC-CO_2,[209] it was demonstrated that

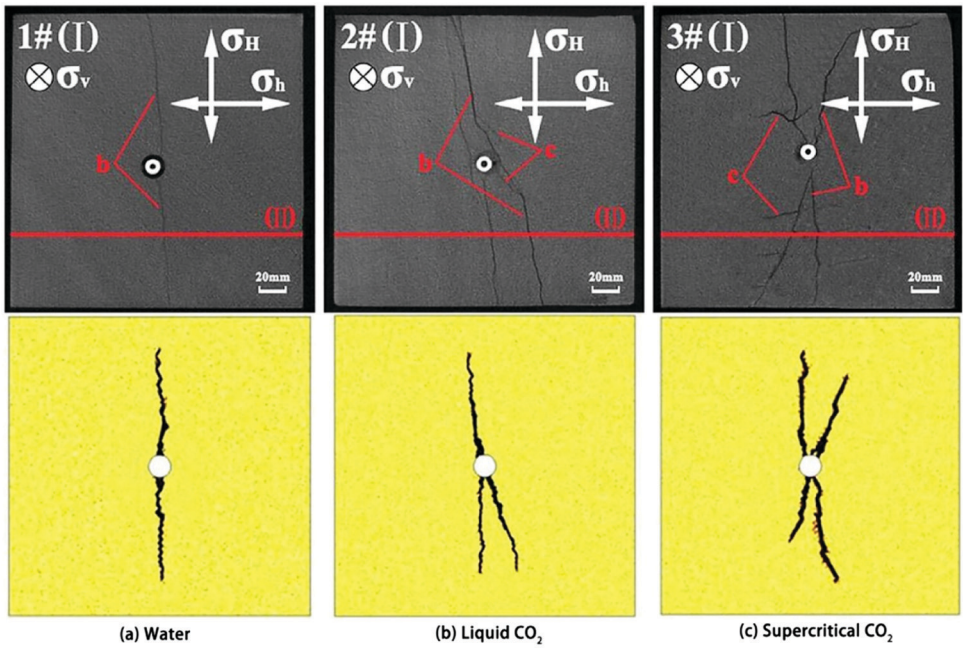

Fig. 6 Fracture matrix created by different fracturing fluids. The upper images are CT scanning results for experimentally fractured Lower Silurian Longmaxi Formation shale cubes with sizes of 200 mm × 200 mm × 200 mm (σ_H (= 10 MPa) and σ_h (= 8 MPa) mean the horizontal principal stresses, σ_v (= 12 MPa) mean the vertical injected stress, b and c mean different types of fractures),[210] the lower images are numerical results with the same boundary conditions.[211]

SC-CO_2 has the lowest and viscous oil the highest breakdown pressure. Fernandez, *et al.*[165] used numerical and experimental methods to investigate the fracability of a CO_2-reactive polymer (CO_2 + nontoxic poly(allylamine)). They found that this nontoxic SC-CO_2-based fracturing fluid could be used to fracture rock cores at lower net pressures, which was caused by the CO_2-triggered volume expansion and the reduction in pore invasion pressure caused by the lower interfacial tension. Zhang, *et al.*[210] found that SC-CO_2 fracturing was more likely than hydraulic fracturing to create fractures, especially secondary fractures near the tail end of the transverse fractures that connect with natural fractures and bedding planes to form a more complex and interconnected fracture network. These results were confirmed by using coupled modelling to simulate shale fracturing using SC-CO_2, liquid CO_2, and water (Fig. 6).[210,211] SC-CO_2 fracturing can create rougher and more complex fracture surfaces than hydraulic fracturing, resulting in higher tortuosity of fractures created by SC-CO_2 compared to freshwater (Fig. 7).[212–215] While keeping the fracturing conditions the same, SC-CO_2 induced an artificial fracture area, which was 60% higher than that induced by hydraulic fracturing.[213] In addition, the fractal dimension of SC-CO_2 induced fracture surface ranged from 2.2314 to 2.2660, higher than that of the water fractured surface (ranged from 2.0855 to 2.1058),[215] indicating more complex rough surfaces. Generally, shale is an anisotropic sedimentary rock with geomechanics and transport properties varying significantly in the horizontal compared to the vertical direction. As such, the orientation of bedding related to the vertical load affects fracture propagation.[77] It was found that the breakdown pressure with SC-CO_2 fracturing was higher than that with freshwater fracturing when the bedding plane orientation varied from 0° to 90°.[212] The reservoir stress and temperature, which also affect the fracturing characteristics, have been investigated by some researchers.[78,216,217] The increase of temperature reduced the viscosity of SC-CO_2 which can easily permeate into the microcrack tip and promote fracture propagation. The SC-CO_2 flow in newly created void fractures will enhance fracturing because of the thermo-mechanical effects caused by the Joule-Thompson throttling process.[218]

Similar to N_2, the low viscosity of SC-CO_2 limits its transport capacity for proppants. However, SC-CO_2 is a good solvent for synthetic polymers,[219] which allows the viscosity to be modified by adding CO_2-philic chemicals (*e.g.* fluoroether disulfate telechelic ionomer) to enhance proppant lifting, transport and delivery under borehole conditions.[22,220,221] The composition of the natural gas in shale reservoirs, specifically its natural gas liquid concentrations, is also likely to impact the physical properties of SC-CO_2 injected into gas-rich formations. For example, varying concentrations of methane, ethane, propane and nitrogen are known to impact the minimum miscibility of CO_2-rich fluids with oil[222] and are likely to impact SC-CO_2 properties as it penetrates into a shale gas formation.

Field tests conducted in the Yan-2011 shale gas well in China showed that SC-CO_2 fracturing was able to create a more complex fracture network than hydraulic fracturing.[223] However, field tests for SC-CO_2 fracturing are still limited. The microseismic response distributions after SC-CO_2 fracturing

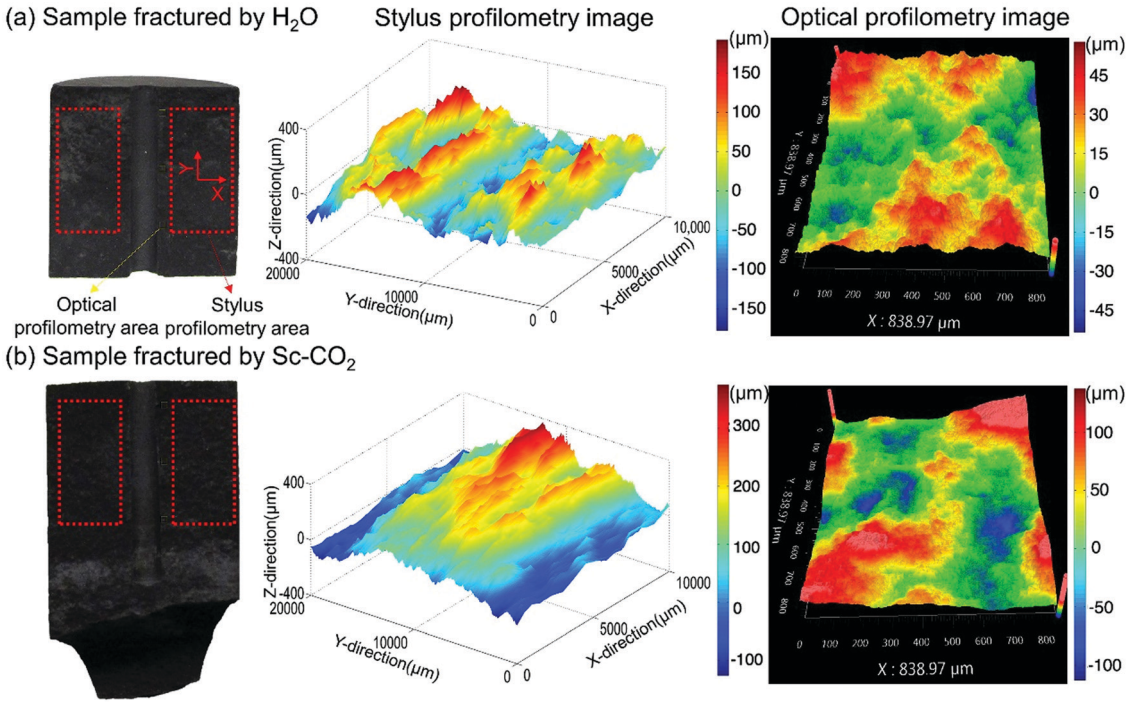

Fig. 7 Surfaces of fractures created by water (a) and SC-CO_2 (b).[215] The stylus profilometry scan focused on an area of 20 mm × 10 mm (red line) and the optical profilometry scan focused on an area of 838.97 μm × 838.97 μm (yellow line).

need to be mapped and evaluated in more detail for a range of shale formations to better define the fracture network development potential SC-CO_2 fracturing.[21] Further field-scale studies are required to obtain additional information on actual shale gas recovery from real anisotropic shale formations, not just laboratory tests.

4.3 CO_2 storage in shale gas reservoirs

When injected into shale gas reservoirs, CO_2 is preferentially adsorbed over methane on organic and inorganic pore surfaces, resulting in methane desorption and CO_2 storage within these formations. In addition, natural and induced fractures offer additional volumes for CO_2 storage, in combination making shale gas reservoirs a potential sink for CO_2 sequestration.

Godec, *et al.*[32] estimated the theoretical CO_2 storage capacity in the Marcellus shale in the Eastern US at >915 m depth. Considering reservoir properties (depth, thickness, total organic carbon, effective porosity, apparent gas saturation, CO_2 and methane adsorption isotherms, and permeability), the adsorbed CO_2 storage capacity is about 0.92 million tons per square kilometer (Mt per km^2). Based on the statistical data from the US Energy Information Administration (EIA) which assesses the technically recoverable shale gas resource around the world,[224] nearly 70 types of shale gas formations from 48 shale gas basins in 32 countries represented primary gas productions ranging from 20% to 35%. The reservoir characteristics of the Marcellus shale are similar to the shale gas basins with an average production of 25%. Assuming an additional 7% of shale gas production enhanced by CO_2 injection, the total shale gas production for Marcellus shale is 32%.[32] As such, it can be calculated that nearly 55 Gt of CO_2 could potentially be sequestrated in the Marcellus shale. This CO_2 storage capacity is 1.7 times larger than the world's CO_2 emissions in 2019. In additional to the Marcellus shale, other shale formations such as the Barnett Shale in the US, the Montney Shale in Canada, and the Longmaxi shale in China which also show considerable technically recoverable shale gas resources, could potentially be used to sequestrate substantial quantities of CO_2. It was therefore concluded that the potential of CO_2 storage in shale gas reservoirs can fulfill the target of reducing 14% of CO_2 which is and will be produced before 2050.[124]

The sustainability and safety of geological CO_2 storage in shale reservoirs are the most important issues requiring careful assessments. The CO_2 trapping mechanisms in saline aquifers are structural and/or stratigraphic trapping, residual (capillary) trapping, solubility trapping, and mineral trapping.[225] However, adsorptive trapping plays a significant role in shale gas reservoirs due to their high clay and organic matter contents, providing significant internal surface area.[226–228] simulated the feasibility of CO_2 storage in the New Albany Shale and found that more than 95% of the injected CO_2 was stored in the form of sorbed gas. As methane can be safely stored in the shale reservoir for long periods of time, the adsorption of CO_2 is also expected to be safe and stable and CO_2 has the potential to penetrate some of the nano-pores that hydrocarbon gases are unable to reach. This property is already exploited in gas adsorption studies to measure the nano-porosity distributions of shale. Liu, *et al.*[229] solubility trapping and mineral trapping are more effective over longer timescales.[230] However, the

matrix swelling and mineral dissolution that cause permeability variations strongly affect the cap sealing performance.[231–233] The risk that some shale reservoirs may not be sealed adequately to prevent long-term seepage of CO_2 needs to be carefully evaluated in detail for each formation and potential trap. To date studies addressing long-term seepage of CO_2 from shales are limited.

5 Concerns of SC-CO_2 enhanced shale gas recovery and sequestration in shale gas reservoirs

5.1 Diffusion and adsorption of CO_2 in shale gas reservoirs

5.1.1 Advective and diffusive flow in shale gas reservoirs. The Knudsen number (Kn) is a commonly used parameter to classify flow regimes in porous media.[234,235] It is a dimensionless parameter, which is defined as the ratio of the molecular mean free path of gas and the characteristic pore size. Accordingly, continuum, slip, transition, and Knudsen flow can be distinguished as summarized in Table 5.

Typically, shale formations are multi-scale porous media, particularly thermally mature organic-rich shales. The space for gas storage and migration within shale reservoirs varies from meter scale to nanometer scale (Fig. 8). At the reservoir scale, gas moves through the reservoir (through the matrix and along connected fracture networks) and eventually flows into the wellbore due to pressure gradients. At the mesoscale, free gas in hydraulic fractures, natural fractures and macropores migrates following Darcy's law. At the microscale, the slippage effect and Knudsen diffusion become significant, because at that scale continuum assumptions for the pore space are partly invalid. At the nanoscale, gas adsorption and desorption and surface diffusion are primary mechanisms controlling gas migration.[237,238] Certain gases such as CO_2 and He, due to their molecular structure and size enter and move more easily than others at the nanopore scale. In adsorption tests on organic-rich shales with abundant nanopores, CO_2 and CH_4 penetrate the nanoscale pores more easily than N_2.[229]

(1) Stress sensitivity effect. During shale gas production, the effective stress of the formation will increase continuously due to a reduction in pore fluid pressure. At higher effective stresses, hydraulic fracture apertures decrease, resulting in a decrease in fracture transmissivity.[239,240] Therefore, understanding the permeability variations of shale gas reservoirs in terms of effective stress is essential for long-term shale gas production, especially for stress-sensitive formations.[241] To accurately estimate formation properties and shale gas production forecasts, various studies report permeability models coupled to mechanical effects.[242–247] Liehui, *et al.*[238] compared the different models and found that the Palmer and Mansoori[248] model is suitable to describe permeability variations of a shale gas well over its entire production life span. Because of gas desorption in shale gas reservoirs, shale matrix shrinkage progressively occurs but particularly during the late production stage which can lead to an increase in permeability.[238]

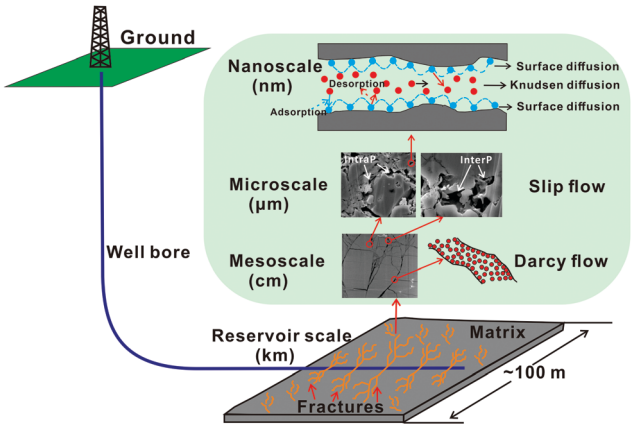

Fig. 8 Gas storage and migration in shale reservoirs occurs at multiple pore scales with at least four distinct flow and gas movement mechanisms involved.

(2) Slippage effect. In conventional oil and gas reservoirs, fluid flow can be described according to Darcy's law where it is assumed that fluid flow occurs in an unimpeded continuum. However, in shale gas reservoirs, micropores and nanopores account for a non-negligible percentage of the total pore volume. At depth, gas flow paths in micropores are comparable to the gas mean free path length. Darcy's law, therefore, needs to be modified in such media because the continuity assumption is invalid.

According to the continuity assumption, the velocity of gas on the pore wall is zero. However, in micropores or nanopores, a non-zero molecular velocity should be considered at the pore wall, which is called the slippage or Klinkenberg effect. The slippage effect strongly affects the gas flow in shale reservoirs. Therefore, theoretical and experimental studies have been performed to describe the gas flow behaviors[242,249–251] and a comprehensive summary is provided in Liehui, *et al.*[238] There,

Table 5 Flow-regime classifications based on Knudsen number[236]

Flow regime	Knudsen number	Description
Continuum (viscous) flow	Kn < 0.01	Darcy's equation for laminar flow, Navier–Stokes equations for turbulent flow
Slip flow	0.01 < Kn < 0.1	Darcy's equation with Klinkenberg correction
Transition flow	0.1 < Kn <10	Darcy's law with Knudsen correction[a]
Knudsen's (free molecular) flow	Kn >10	Knudsen diffusion,[b] usually occurs in nanopores

[a] The details for Knudsen correction are provided in ref. 236. [b] The details for Knudsen correction are provided in ref. 237.

it was pointed out that the two most commonly used methods for modeling gas flow including slippage are an empirical Klinkenberg correction and slippage modification based on slip boundary conditions. For the empirical Klinkenberg correction, the intrinsic permeability is corrected by an equation that includes pore pressure, the slippage factor, and apparent permeability.[252] For the slip boundary conditions, the first order, second (or higher) order and Langmuir slip boundary conditions are used to describe the gas flow in a transitional flow regime.[253,254]

5.1.2 Sorption capacities and competitive adsorption of CO_2 *versus* CH_4

5.1.2.1 Shale gas sorption capacities. Shale gas is commonly stored in reservoirs as dissolved gas, in the sorbed and in the free gas state. Sorbed gas accounts for 20 to 85% of the total shale gas storage capacity[255] and is therefore important in the shale gas resource assessment. The gas sorption capacity of shales has been widely recognized as being closely related to moisture content, surface area, pore size distribution, total organic carbon (TOC) content, organic matter type and maturity, as well as clay mineralogy and clay content.[256–262]

TOC content is considered the most significant control on methane sorption capacity.[263–265] Organic matter, typically quantified as TOC, is the source of the hydrocarbon gases present in a shale, while gas generation is mainly controlled by temperature and time during burial. Micropores in organic matter (<2 nm) provide high specific surface areas in comparison to macropores (>50 nm), particularly in thermally mature shales.[261,266] Therefore, the methane sorption capacity correlates positively with TOC.[259,267] Organic matter type and thermal maturity play complex roles in methane sorption capacity. For gas shales in the gas window, the sorption capacity shows a positive relationship with maturity because microporosity increases with maturity. Source rock organic matter can be classified in three types, which are found to generally show different sorption capacities, with Type I (lacustrine) < Type II (marine) < Type III (terrestrial).[268] The micropores in clay minerals are also able to adsorb significant amounts of methane. For clay-rich shale, the methane sorption capacity can significantly contribute to the total sorption capacity.[261,269–271] found that different types of clays have different sorption capacities: smectite ≫ mixed layer illite/smectite > kaolinite > chlorite > illite. Busch *et al.* found a similar relationship with smectite > illite > kaolinite > chlorite.[226] It should be noted that although water has a negative effect on the sorption capacity,[272] most sorption tests have been carried out on dry samples which are not representative of reservoir conditions and should be treated carefully.

5.1.2.2 Competitive adsorption of CO_2 versus CH_4. While injecting CO_2 into shale reservoirs for gas recovery and CO_2 sequestration, the sorption ability of CO_2 in shales should be considered. Various studies investigated the CO_2 adsorption capacity of shales and clay minerals.[30,226,273–278] They all found that the sorption capacity of CO_2 in shale samples was higher than for CH_4. The CO_2/CH_4 sorption ratio ranges between 1.3 and 10 for dry shale samples (Fig. 9).[276] The molecular diameter of CO_2 (0.33 nm) is slightly smaller than for CH_4 (0.38 nm), which allows access to narrower pores and therefore higher surface area. In addition, CO_2 has a higher sorption enthalpy resulting in a higher sorption capacity of CO_2 over CH_4.[227,279]

In the process of CO_2-enhanced shale gas recovery, the competitive adsorption of CO_2 and CH_4 are essential to understand the efficiency of shale gas recovery and CO_2 storage.[30] Various studies report experimental CO_2–CH_4 competitive adsorption in shale samples.[33,280–287] Here, shale samples are pressurized with CO_2 and CH_4 mixed gases at different molar ratios. With the increase in saturation pressure, the sorption volume of CO_2 increases, while the sorption volume of CH_4 decreases.[281] As shown by nuclear magnetic resonance (NMR) studies, CO_2 competitively sorbs over CH_4.[281] With an increase in reservoir pressure, CO_2 shows better sorption ability than CH_4.[281,283,288] However, CO_2 enhanced CH_4 extraction exists in an optimal pressure range. In the study of Lee, *et al.*,[289] the suggested pressure range was 7 to 9 MPa. Other factors such as pore volume and pore size distribution (PSD), also affect shale sorption capacity.[283]

5.2 CO_2–shale or CO_2–liquid–shale interactions

When CO_2 is injected into shale gas reservoirs, geochemical CO_2–water–rock interactions occur over a period of time. This might cause physical properties of shale to change, potentially affecting the shale gas recovery efficiency and CO_2 storage process.

5.2.1 Carbonic acid in water + CO_2. The dissolution of gaseous CO_2 in water creates a weak carbonic acid (H_2CO_3), which is in dynamic equilibrium with its dissociated forms (HCO_3^- and CO_3^{2-}).[290–293] The microsolvation of H_2O and CO_2 and the formation/decomposition of carbonic acid have been extensively studied by means of density functional theory (DFT), Hartree–Fock (HF), *ab initio* molecular dynamics, matrix isolation IR experiments, phase molecular beam, *etc.*[293–298] However, the widely accepted reaction between H_2O and CO_2 in gaseous and aqueous conditions may be different in SC-CO_2. The structural feature of SC-CO_2 is that each CO_2 molecule is surrounded by six other CO_2 molecules configured in a distorted T-shaped configuration around the carbon.[299] The reaction between H_2O and CO_2 to form H_2CO_3 in supercritical condition has a higher barrier than that of gaseous condition because H_2O has to displace the surrounding CO_2 molecule's out of their equatorial positions and align them with the reacting C.[293,298] Glezakou, *et al.* used an *ab initio* molecular dynamics method to examine the structure, dynamics, and vibrational spectra of SC-$CO_2/(H_2O)_n$ (n = 0–4).[298] They found that the strongest interactions between SC-CO_2 and H_2O occur in the case of monomeric water. The dynamic hydrogen bonds with the oxygens are mostly formed between the equatorial and polar coordinating CO_2 molecules. For the decomposition of H_2CO_3, the enthalpy and entropy terms are similar in SC-CO_2, but that is not the case for gaseous CO_2. The formation of H_2CO_3 in SC-CO_2 is thermodynamically unfavorable. Once formed, H_2CO_3 will probably be the

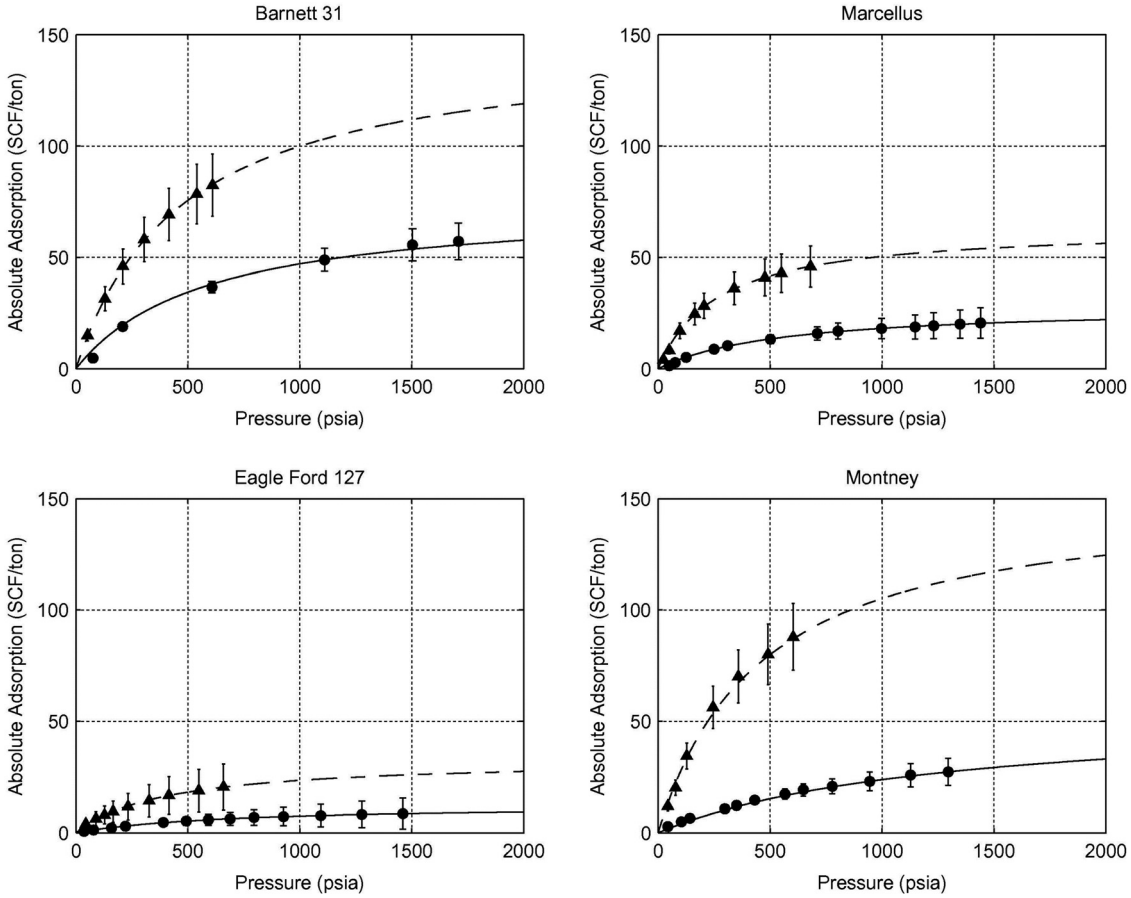

Fig. 9 Methane and carbon dioxide adsorption isotherms on samples from the Barnett, Marcellus, Eagle Ford and Montney shale reservoirs (triangular point-CO_2, dot-CH_4, line-model fitting).[30]

undissociated form while the water is likely to remain unsaturated.[293] The low solubility of water in SC-CO_2 resulted in the water clustering when the water concentration in SC-CO_2 was high. In the reservoir condition, the water usually contains brines like NaCl, the formation/decomposition of carbonic acid will be more complex and need further investigation.

5.2.2 Chemical reactions. Although well-defined concepts in aqueous solutions such as mineral solubility and ion activity do not have corresponding thermodynamic meaning in water-based SC-CO_2, McGrail, *et al.*[171] demonstrated that water-based SC-CO_2 can be reactive with different mineral phases. Many scholars have proved the mineral dissolution and precipitation in such acidic fluids.[300–302] Busch, *et al.*[226] investigated the CO_2-shale interactions with temperatures between 45 °C and 50 °C and pressures up to 20 MPa. Minor geochemical reactions such as the dissolution of silicates and precipitation of carbonates were observed after sorption experiments. Alemu, *et al.*[303] selected two caprock shale samples (a carbonate-rich and a clay-rich shale) to study the reactions between rocks and a mixture of brine and SC-CO_2 (the pressure was 11 MPa, the temperature ranged from 80 to 250 °C). By analyzing fluid major element concentrations as well as SEM and XRD tests, they indicated dissolution and re-precipitation of carbonates, dissolution of plagioclase, illite, chlorite and the formation of smectite. When shale rocks are exposed to CO_2–water mixtures, chemical reactions such as the dissolution of calcite, carbonates and clay minerals could be observed.[304] If the imbibition time is long, quartz could also be dissolved.[305] The geochemical reactions can potentially affect petrophysical properties which will be discussed below.

5.2.3 Physical changes. Mineral dissolution creates additional porosity within rock formations, whereas precipitated minerals can block the connection of pores. These chemical processes can change the petrophysical properties of shales. Therefore, investigating shale properties following CO_2–water–rock interaction can help predicting potential causes and consequences over long timescales, using advanced experimentation and reactive transport or batch modelling. This will promote the assessment of the suitability for CO_2 enhanced shale gas recovery and CO_2 sequestration of specific shale gas reservoirs. In the following, the macro and microscale changes of shale properties after reaction with CO_2 and carbonated fluids are reviewed.

5.2.3.1 Macroscale variations. Important macroscale properties of shales include mechanical (strength, brittleness, hardness/toughness) or petrophysical properties (permeability, porosity). Significant changes of these properties due to

Table 6 Experimental studies of shale strength affected by imbibition of CO_2 and CO_2-based fluids subjected to different conditions and methods

Rock type	Soaking fluids	Soaking time	Temperature and pressure	Testing method
Longmaxi shale[306–308]	CO_2 CO_2 + water CO_2 + NaCl (20% wt)	10/20/30 days	40 °C, 7 MPa 40 °C, 9 MPa	UCS tests
Longmaxi shale[309]	CO_2	10 days	38 °C, 4/6/8/12/16 MPa	UCS tests
Longmaxi shale[310]	CO_2 CO_2 + NaCl (10% wt)	7 days	45 °C, 6 MPa 45 °C, 12 MPa	UCS tests
Longmaxi shale[311]	CO_2	10/30/60 days	40 °C, 10 MPa	TS tests
Longmaxi shale, Lujiaping shale[312]	CO_2 + brine (KCl 2.0%, NaCl 5.5%, $MgCl_2$ 0.45%, $CaCl_2$ 0.55% wt)	7 days	80 °C, 20 MPa	TS tests

CO_2–water–rock interactions might impact reservoir performance in terms of mechanical stability and recovery rates.

(1) Mechanical properties. Strength is a fundamental mechanical property of a rock. Previous studies report uniaxial compressive strength (UCS) and tensile strength (TS) tests to determine the variation of a shale's strength after CO_2–water–rock reaction. The experimental conditions and major results are shown in Table 6 and Fig. 10.[306–312] It can be seen that CO_2 and its saturated fluids decrease the strength of shale samples. With 30 days of imbibition, the strength of shales reacted with sub/supercritical CO_2, sub/supercritical CO_2 + water, and sub/supercritical CO_2 + brine decreased by 20% and 30%, 56% and 66%, and 61% and 70%, respectively. Longer imbibition time leads to more extensive CO_2–shale or CO_2–water/brine–shale reactions and a higher reduction of stress. With a lower pH value than pure CO_2, CO_2 saturated water or brine yields conditions where chemical reactions are more violent.[313] Therefore, the strength of shale samples with CO_2 + water/brine imbibition is lower than that with CO_2 imbibition. SC-CO_2 has no capillary force and lower values of viscosity than subcritical CO_2. With the same reaction time, SC-CO_2 penetrates into shale samples and reduces their strength more than subcritical CO_2. The trends of strength variation vary among shale types. Different shales have distinct anisotropy, mineral composition, and thermal evolution, which leads to differences in the mechanical changes caused by CO_2 and CO_2 + water/brine imbibition.

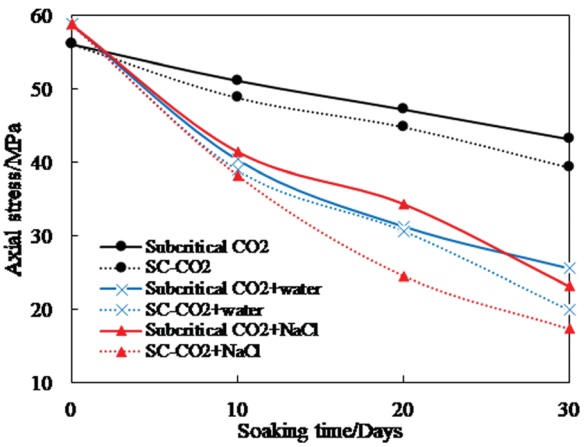

Fig. 10 Compressive and tensile stress of shale samples after CO_2 and CO_2 saturated water or brine imbibition.[306–308]

The shale–CO_2 or shale–water/brine–CO_2 interactions influence the brittleness index (BI) of shale. BI is usually used to characterize the potential of fracability, that is, a higher value BI means a better fracability, which is beneficial for reservoirs with re-fracturing treatment. Lyu, *et al.*[314] used the energy-based method to calculate the BI values of shale samples with different soaking times in subcritical CO_2, SC-CO_2, subcritical CO_2 + water, and SC-CO_2 + water. The results showed that, with 30 days of imbibition, subcritical CO_2 and SC-CO_2 imbibition resulted in 13% increase of the BI values of shale, while samples with subcritical CO_2 + water and SC-CO_2 + water imbibition displayed 17% reduction of BI values. It can be deduced that CO_2 imbibition enhances a shale's fracability, while CO_2 + water imbibition lowers the fracability. The fracability can also be characterized by the variations of toughness and hardness. If the toughness decreases, the brittleness increases. A low value of hardness means fractures can be created more easily. Based on the study of Ilgen, *et al.*,[315] with 7 days of CO_2–brine imbibition, quartz-rich shales showed a small decrease, while dolomite- and muscovite-rich shales showed about 50% decrease in toughness and hardness. However, the fracability of shale reservoirs cannot be determined using BI, toughness, or hardness alone. As reported in Lyu, *et al.*[306] and Lyu, *et al.*,[307] samples soaked in CO_2 + water were weakened more than those soaked in CO_2. The weakening of shale which caused by imbibition induced cracks and pores also contributes to better fracability.

As discussed before, four types of gas flow should be considered when CO_2 is injected into shale reservoirs: viscous flow, Knudsen diffusion, molecular diffusion, and surface diffusion.[316–319] Shale–CO_2 or shale–water/brine–CO_2 reactions change the porosity and pore size distribution of shale, which potentially influence the dominant flow mechanisms in shale pores and alter the permeability.[320,321] Kim, *et al.*[322] simulated the SC-CO_2 flooding and "huff and puff" process to elucidate the effects of CO_2 injection for enhancing gas recovery and CO_2 storage. The results showed that SC-CO_2 injection enhances CH_4 production because reactions with CO_2 caused shale deformation and an increase in permeability. Zou, *et al.*[312] tested the permeability variations of the Liujiaping (LJP) shale and Longmaxi (LMX) shale after soaking in CO2 + brine for

different reaction time, temperature, and pressure. They found that the permeability of both shales increased with increasing reaction time, temperature, and pressure. This was caused by the dissolution of carbonates, which creates more pores and improved pore connectivity.

However, the experiments conducted by Zhou, *et al.*[323] showed that CO_2 adsorption leads to shale swelling and a decrease in permeability. The permeability reduction is more likely to occur in ultra-low permeability shales where fluids flow paths are more sensitive to CO_2 sorption-induced swelling.[324]

The published experimental results, therefore, provide complex results suggesting that permeability of shale after CO_2 and CO_2 based fluids imbibition can either increase or decrease depending on shale properties and a range of factors. The complex trends are not just affected by the processes of adsorption/desorption and dissolution/precipitation. The composition of the samples and the bedding angles, testing methods, and imbibition conditions are also important factors. The salinity of the formation fluids and the temperature of the injected SC-CO_2 fluids impact interfacial tension (IFT) of the shale–water/brine–CO_2 solutions in the reservoir, which in turn impacts the relative permeability of the water/brine–CO_2-rich phase *versus* the hydrocarbon-rich phase in the reservoir.[325] More experimental and analytical studies are required to better quantify and rank the significance of these factors on permeability changes in a wide range of shales following SC-CO_2 imbibition.

5.2.3.2 Microscale variations. The macroscale changes of shale are accompanied by microscale variations. Pore sizes of microporous systems like gas shales are classified into three distinct groups: micropores (<2 nm), mesopores (2–50 nm), and macropores (>50 nm).[326,327] CO_2, with linear molecular geometry, can access a certain fraction of micropores that other naturally-occurring gases cannot access. Jiang, *et al.*[328] experimentally investigated the microstructure of shales after treatment with SC-CO_2 at different pressures (8–18 MPa), reaction times (0–5 days) and temperatures (40–90 °C). The specific surface area and porosity increased slightly with an increase in temperature and reaction time. Higher pressure significantly promoted an increase in specific surface area and porosity. Similarly, the increasing trends of porosity have also been observed in shales with SC-CO_2 saturated brine imbibition.[312] Pan, *et al.*[329] used marine and terrestrial shale samples to conduct similar tests but increased the soaking time to 14 days. After SC-CO_2 imbibition, the number of micropores and mesopores in the marine shale (with low clay contents) decreased, while the number of macropores increased, resulting in a higher porosity overall. However, the terrestrial shale with high clay content exhibited the opposite trend of porosity changes to the marine shale after SC-CO_2 imbibition. This was interpreted to be mainly caused by clay swelling during imbibition.

The increase in porosity occurs mainly because of the chemical reactions between CO_2/CO_2-based fluids and shale minerals during the process of fracturing and sequestration. The dissolution of calcite, quartz, illite/smectite, and chlorite and the precipitation of iron-rich carbonate(siderite), illite, and smectite have been observed when shale samples are exposed to CO_2.[330–333]

5.3 Further concerns

5.3.1 Costs of using SC-CO_2 in shale gas recovery. During the process of SC-CO_2 enhanced shale gas recovery, the CO_2-related costs are related to CO_2 capture, transport, and storage. CO_2 can be obtained from power plants and transported by pipelines, trucks or ships.[334,335] Pipeline corrosion caused by CO_2 can be prevented by surface coating and cathodic protection.[336] CO_2 should be compressed to a liquid phase which can be stored near the well. For SC-CO_2 fracturing, CO_2 will be compressed to a high pressure and injected into shale wells. The energy requirement for CO_2 compression is about 1.2 to 1.5 kW h per t-CO_2 per 1 MPa.[337,338] The flowback gas which mixes with natural gas and CO_2 need to be separated. The CO_2 content in natural gas should be decreased to 2–5% to meet typical pipeline specifications.[339] The major separation processes of CH_4 and CO_2 are chemical and physical adsorption, low temperature distillation, and membrane separation.[340] Membrane separation represents commercial advantages and has become a major industrial application.[341] The cost of the gas separation system is not a one-time investment, the operation and maintenance cost, the natural gas lost, and the gas processing cost should also be considered.[342] The separated CO_2 can be reused for fracturing. The cyclic injection process should be optimized based on the net present value (NPV).[343]

Currently, the investments required for SC-CO_2 fracturing are significantly higher than for hydraulic fracturing. However, if the SC-CO_2 fracturing process is combined with CO_2 sequestration, costs can be lowered when the operation is part of a CO_2 tax scheme. Shafeen, *et al.*[344] calculated the investment of a CO_2 sequestration project. A total of US$257 million dollars is needed for a project with 1 off shore platform, 10 injection wells, and 112 kilometers of pipelines, the CO_2 capture costs ranging from US$30 per ton to US$60 per ton, are not included.[345] For hydraulic fracturing, the total costs of disposal, basic separation, and desalination of flowback water range roughly between $78 000 and $1 460 000 for each well.[346] The costs for groundwater and surface water cleanup add significant expenses to this operation.[347] Till now, hydraulic fracturing is till the appropriate technique for shale gas recovery. The application of SC-CO_2 fracturing together with CO_2 sequestration relies on the supporting policy from the government, more capital channels, and the integration of social resources.

5.3.2 Induced seismicity and environmental impacts. Similar to hydraulic fracturing, extracting hydrocarbons from low permeability shale formations through SC-CO_2 fracturing may also cause environmental impacts and induce or trigger earthquakes. During the fracturing process, SC-CO_2 can penetrate the unconnected micropores in the formation more easily than the water-based fracturing fluid, form a high pore pressure area around the wellbore, and may transfer the fluid pressure to the farther and deeper part of the formation. Numerous

experimental studies and a few field tests have shown that SC-CO_2 fracturing can generate more micro-fractures and micro-seismic events compared to hydraulic fracturing.[210,348,349] In addition, characteristics of SC-CO_2 under reservoir conditions may accelerate the reactivation of pre-existing faults, especially considering the potential phase changes. For instance, SC-CO_2 will be converted to gaseous CO_2 when the pressure decreases and suppress dilatancy hardening, which may promote the stable or aseismic slips along pre-existing faults.[350] Besides, SC-CO_2 fracturing tends to induce extensive three-dimensional cracking and shear dominant fracture due to the lower viscosity of SC-CO_2 than water in this perspective. The risk of felt seismicity when using CO_2 as a fracturing fluid or in CO_2 sequestration might therefore be a considerable concern.

So far, studies investigating the environmental impacts of field SC-CO_2 fracturing are still missing in the literature. CO_2 is stable, non-flammable, and easy to be recycled. As an environmentally-friendly fluid, the use of (SC-)CO_2 in shale gas recovery should lower environmental impacts (*e.g.*, water contamination issues), especially considering the potential for CO_2 sequestration both during and after the stimulation phase. However, CO_2-based fracturing will definitely have an impact on the reservoir environment. Water in the formation will tend to dissolve in the SC-CO_2, and the remaining brine will become supersaturated with dissolved salts and precipitation may occur.[22] Precipitation of mineral salts could lead to the blocking of small pores in the reservoir and undesirably restrict subsequent extraction of the hydrocarbons.

5.3.3 Life cycle assessments of CO_2-based fracturing. Despite the concerns of costs and environmental impacts, life cycle assessments (LCA) of using SC-CO_2 in shale gas recovery are necessary to quantify the challenges and opportunities that meet the industry and environmental protection goals. Wilkins, *et al.*[351] systematically compared the life cycle energy use, greenhouse gas emissions, and water consumption of unconventional gas recovery between hydraulic fracturing fluid and CO_2-based fracturing fluid. Because of the gas compression, separation, transportation, and energy losses for flaring, the net energy impact of CO_2-based fracturing was 44% higher than that of water-based fracturing. While considering the increase of energy production, the net energy impact of CO_2-based fracturing only accounted for two thirds of the water-based fracturing. It is worth noting that CO_2-based fracturing achieved net carbon offsets as shale pores show considerable adsorption capacity of CO_2. Water-based fracturing consumes large amount of water. The transfer to CO_2-based fracturing avoids high-volume surface and groundwater extractions and further minimizes active fluid management over the well's lifetime, including produced water storage, transport, and treatment at the wellhead. CO_2-based fracturing is region-specific. It is much more suitable for regions where the extractions and disposal of high volumes of water are constrained and CO_2 sources are accessible.

The public concerns of hydraulic fracturing focus on the large amount of water consumption, drinking water contamination, fugitive methane emissions, seismic events, noise pollution, and truck traffic.[7,352] Although CO_2-based fracturing avoids water consumption and contamination, the increase of total truck trips (100% higher than water-based fracturing) will lead to high public health risks. The construction of CO_2 pipelines can help to reduce the risks and increase the fluid transport efficiency. Depleted shale well can be used for CO_2 sequestration. A design of collocated parallel pipelines for both CO_2 and natural gas transport is beneficial for CO_2 fracturing/sequestration and natural gas supply.[353] The advanced pipeline strategy requires the coordination between CO_2 sources, field services suppliers, and producers. Although CO_2-based fracturing shows advantages for shale gas recovery, the effective large-scale deployment of this technique should consider social, technical, and environmental trade-offs.

5.3.4 Further investigations

5.3.4.1 Laboratory study. Previous work has shown some advantages of SC-CO_2 enhanced shale gas recovery. However, the changes to shale properties, fracturing results, and drilling ability after imbibition with CO_2 or CO_2-based fluids are complex. Generalization of established trends is not yet possible using information from studies published to date. This is because the laboratory tests are limited by several factors:

(a) Sample anisotropy. With the process of deposition, burial, and lithification, shale can be divided into three types: marine shale, continental (lacustrine) shale, and transitional facies shale. The mineral composition and porosity of the three types of shales are different, which results in variable adsorption abilities.[261,354] Even for one type of shale, the clay minerals assemblage can vary by location. The methane adsorption ability of each clay mineral assemblage tends to be different (*e.g.*, where smectite $\gg$ illite compared to smectite mixed layers $>$ kaolinite $>$ chlorite $>$ illite).[355] Therefore, it is necessary to determine the types of shale and characterize its clay mineralogy and heterogeneity before imbibition tests.

(b) Sample Size effect. The mechanical properties of rocks are closely related to the size (diameter, height-diameter ratio) of samples.[356] The bedding angles of shale formations also affects rock properties.[357] More importantly, the size scale of samples used in laboratory tests is typically too small to reliably represent the real reservoir conditions. Therefore, comparisons of reaction results between samples with different sizes are necessary. Despite the difficulty of sample preparation, large shale samples are suggested for conducting robust SC-CO_2 imbibition tests.

(c) Reaction conditions. The CO_2 injection and release rate, the heating rate, and the pressure/temperature stabilization in the imbibition process affect the actual sample test results. The soaking time in most published studies was less than 30 days. According to some published research,[358,359] 30 days of imbibition is not long enough to affect the porosity of shale or coal. A shale gas well might remain productive for 5 to 40 years, and CO_2 sequestration needs to be stable for thousands of years. While the diffusion of CO_2 in shale rocks is as slow as millimeters per year. Therefore, to better understand the effects of SC-CO_2 on shale reservoirs, longer soaking times in laboratory tests are required.

5.3.4.2 Field tests. Previous studies mainly focus on the laboratory tests of the possibility of using SC-CO_2 for shale gas recovery. Field tests for SC-CO_2 fracturing are still limited. More investigations should be conducted by field tests to promote the application of SC-CO_2 enhanced shale gas recovery. (a) Drilling. Laboratory tests have demonstrated the feasibility of SC-CO_2 based drilling. However, in the real condition of application, the drilling ability should consider both the fluids flow in the wellbore and the cutting-carry ability of fragments. The physical properties of SC-CO_2 is sensitive to the pressure and temperature that are related to the CO_2 injection, injection pressure and temperature, depth of the well, and the roughness of the well surface.[360,361] The change of physical properties will directly affect the drilling ability of SC-CO_2. Some researchers have investigated the SC-CO_2 flow by simplified models.[191,362,363] However, these models have not been validated by field tests. To increase the drilling efficiency, the fragments produced by drilling need be cleaned immediately. The cutting-carry ability of SC-CO_2 was studied by laboratory experiments with a meter-scale. While a well for shale gas recovery is usually composed of a vertical well with hundreds of meters to several kilometers and several horizontal wells with more than one kilometer. The cutting-carry ability of SC-CO_2 at a kilometer-scale remains unknow. (2) Proppant-carry in fractures. Like hydraulic fracturing, SC-CO_2 fracturing also needs the proppants to hold the fractures open. However, SC-CO_2 has good diffusion ability, the filtrate loss is larger than using water. Thereby the proppant-carry ability decreases with a decrease in turbulence intensity in fractures. Meanwhile, the particle-fluid multiphase flow is also affected by temperature and pressure variations caused by the heat transfer between shale rocks and SC-CO_2.[364,365] (3) Fracturing equipment. Before fracturing, sands should be continuously be added to the liquid CO_2. It is very difficult to control the high-pressure sand-CO_2 mixing process. Sands in the well can block perforation nozzles resulting in overpressure of the fracturing equipment.[349,366] Therefore, a sand-adding equipment is necessary to fulfil the demand of large-scale SC-CO_2 fracturing.

6 Conclusions, challenges, and perspectives

Based on the review of the current literature, we conclude that it is feasible to use SC-CO_2 to enhance shale gas recovery instead of using conventional water-based fracturing fluids. SC-CO_2 might be applied with three distinct objectives: (1) Drilling. The rock-breaking threshold pressure and cutting energy required for SC-CO_2 jets are lower than those of water jets. However, the capacity of SC-CO_2 to carry cuttings still needs to be improved. (2) Fracturing. SC-CO_2 fracturing can create more irregular multiple fractures and rougher and more complex fracture surfaces than liquid CO_2 or water. (3) Sequestration. Shale gas reservoirs have substantial potential for CO_2 sequestration. CO_2 injected into reservoirs could be safely and stably stored by solubility, adsorption, and mineral trapping. Considering the large quantities of CO_2 consumed during each SC-CO_2 fracture stimulation operation, the large-scale application of SC-CO_2 enhanced shale gas recovery is restricted by the high expense of CO_2 capture and transportation to supply CO_2 to many injection sites.

Although SC-CO_2 shows significant benefits in enhancing shale gas recovery, there are still some challenges that need to be addressed. Firstly, CO_2–shale or CO_2–water/brine–shale interactions strongly affect the properties of shale. The direct and indirect effects of these interactions on the recovery of shale gas and CO_2 sequestration are still unknown. More work is required to better quantify and model such effects. Secondly, the mechanism of SC-CO_2 fracturing is still unclear. The fracturing process is affected by the variations in pressure and temperature, the physical properties of SC-CO_2, the leak-off of SC-CO_2 and the physical and chemical reactions between shale and SC-CO_2. It is totally different from hydraulic fracturing. The numerical simulation methods such as the extended finite element method, boundary element method and other advanced methods can be used together with delicate laboratory tests to reveal the mechanism of fracture initiation and propagation during SC-CO_2 fracturing. Thirdly, more data from field tests is necessary to demonstrate the feasibility of SC-CO_2 enhanced shale gas recovery and CO_2 sequestration in a wide range of potential shale gas reservoirs. The proppant-carry and sand-carry abilities of SC-CO_2 are poor. Proppant and sand could therefore potentially accumulate in the wellbore or the tips of cracks which would be detrimental to perforation and fracturing. The flow resistance of SC-CO_2 in the wellbore and the bit nozzles is very high. To fulfill the injection volume, a higher pumping pressure is therefore needed. This risks causing overpressure in the surface equipment.[349] Moreover, induced-seismicity monitoring is required. This involves multi-disciplinary inputs from geophysics, geology, and reservoir engineering, which are required for advanced identification, processing, and interpretation of induced seismicity. Such monitoring and recorded signal interpretations are essential to ensure the safe and effective production and sequestration of shale gas over long time periods.

Author contributions

Jingqiang Tan conceived the idea and organized writing. Qiao Lyu, Jingqiang Tan, and Yiwen Ju led the preparation of the manuscript. Lei Li, Andreas Busch, David A. Wood, Pathegama Gamage Ranjith, and Richard Middleton helped to revise and edit the article. Biao Shu and Qiao Lyu conducted a literature review of CO_2 emissions and CO_2 capture, utilization, and storage. Chenger Hu helped to summarize the costs of using SC-CO_2 in shale gas recovery and field tests. Zhanghu Wang and Ruining Hu drew and improved some of the figures. All authors contributed to the study with valuable discussions.

Conflicts of interest

There are no conflicts to declare.

Acknowledgements

The authors are grateful for financial support from the National Natural Science Foundation of China (Grant No. 72088101, 41530315, 41872151, 41872160, 42002160, and 42004115), the Strategic Priority Research Program of the Chinese Academy of Sciences (Grant No. XDA05030100) and the Innovation-Driven Project of Central South University (Grant no.: 502501005).

Notes and references

1 EIA, International Energy Outlook, 2019, https://www.eia.gov/outlooks/ieo/pdf/ieo2019.pdf.
2 I. P. o. C. C. (IPCC), *Climate change and land: An IPCC special report on climate change, desertification, land degradation, sustainable land management, food security, and greenhouse gas fluxes in terrestrial ecosystems*, 2019.
3 R. A. Kerr, *Science*, 2010, **328**, 1624–1626.
4 H. Yang and J. R. Thompson, *Nature*, 2014, **513**, 315.
5 J. Yuan, D. Luo and L. Feng, *Appl. Energy*, 2015, **148**, 49–65.
6 E. I. Administration, U.S. Natural Gas Gross Withdrawals and Production, DOI: https://www.eia.gov/dnav/ng/ng_prod_sum_dc_NUS_mmcf_a.htm.
7 A. Vengosh, R. B. Jackson, N. Warner, T. H. Darrah and A. Kondash, *Environ. Sci. Technol.*, 2014, **48**, 8334–8348.
8 D. Alleman, *Hydraulic Fracturing of the Marcellus Shale*, 2011.
9 D. M. Kargbo, R. G. Wilhelm and D. J. Campbell, *Environ. Sci. Technol.*, 2010, **44**, 5679–5684.
10 J. Wang, M. Liu, Y. Bentley, L. Feng and C. Zhang, *J. Environ. Manage.*, 2018, **226**, 13–21.
11 J. P. Nicot and B. R. Scanlon, *Environ. Sci. Technol.*, 2012, **46**, 3580–3586.
12 P. Reig, T. Luo and J. N. Proctor, *Global shale gas development: water availability and business risks*, World Resources Institute, 2014.
13 W. T. Stringfellow, J. K. Domen, M. K. Camarillo, W. L. Sandelin and S. Borglin, *J. Hazard. Mater.*, 2014, **275**, 37–54.
14 R. Jackson, A. Gorody, B. Mayer, J. Roy, M. Ryan and D. Van Stempvoort, *Groundwater*, 2013, **51**, 488–510.
15 K. B. Gregory, R. D. Vidic and D. A. Dzombak, *Elements*, 2011, **7**, 181–186.
16 H. Chen and K. E. Carter, *J. Environ. Manage.*, 2017, **200**, 312–324.
17 E. Rester and S. D. Warner, in *Environmental and Health Issues in Unconventional Oil and Gas Development*, ed. D. Kaden and T. Rose, Elsevier, 2016, pp. 49–60, DOI: 10.1016/B978-0-12-804111-6.00004-2.
18 D. C. DiGiulio and R. B. Jackson, *Environ. Sci. Technol.*, 2016, **50**, 4524–4536.
19 E. E. Yost, J. Stanek and L. D. Burgoon, *Sci. Total Environ*, 2017, **574**, 1544–1558.
20 G. A. Kahrilas, J. Blotevogel, P. S. Stewart and T. Borch, *Environ. Sci. Technol.*, 2015, **49**, 16–32.
21 L. Li, J. Tan, D. A. Wood, Z. Zhao, D. Becker, Q. Lyu, B. Shu and H. Chen, *Fuel*, 2019, **242**, 195–210.
22 R. S. Middleton, J. W. Carey, R. P. Currier, J. D. Hyman, Q. Kang, S. Karra, J. Jiménez-Martínez, M. L. Porter and H. S. Viswanathan, *Appl. Energy*, 2015, **147**, 500–509.
23 C. Fu and N. Liu, *J. Nat. Gas Sci. Eng.*, 2019, **67**, 214–224.
24 D. V. S. Gupta and T. T. Leshchyshyn, presented in part at the SPE Latin American and Caribbean Petroleum Engineering Conference, Rio de Janeiro, Brazil, 2005/1/1/, 2005.
25 Gupta and Bobier, presented in part at the SPE Gas Technology Symposium, Calgary, Alberta, Canada, 1998/1/1/, 1998.
26 S. Meng, H. Liu, J. Xu, Y. Duan, Q. Yang and Z. Yao, presented in part at the SPE Asia Pacific Oil & Gas Conference and Exhibition, Perth, Australia, 2016/10/25/, 2016.
27 Y. Fang, C. Wang, D. Elsworth and T. Ishibashi, *Geomech. Geophys. Geo-Energy Geo-Resources*, 2017, **3**, 189–198.
28 M. K. Fisher, C. A. Wright, B. M. Davidson, A. Goodwin, E. Fielder, W. Buckler and N. Steinsberger, *SPE Annual Technical Conference and Exhibition*, San Antonio, Texas, 2002.
29 V. I. Likhtman, E. D. Shchukin and P. A. Rebinder, *Physicochemical mechanics of metals: adsorption phenomena in the process of deformation and failure of metals*, 1964.
30 R. Heller and M. Zoback, *J. Unconv. Oil Gas Resour.*, 2014, **8**, 14–24.
31 P. Huo, D. Zhang, Z. Yang, W. Li, J. Zhang and S. Jia, *Int. J. Greenhouse Gas Control*, 2017, **66**, 48–59.
32 M. Godec, G. Koperna, R. Petrusak and A. Oudinot, *Int. J. Coal Geol.*, 2013, **118**, 95–104.
33 L. Huang, Z. Ning, Q. Wang, W. Zhang, Z. Cheng, X. Wu and H. Qin, *Appl. Energy*, 2018, **210**, 28–43.
34 D. W. Keith, G. Holmes, D. St. Angelo and K. Heidel, *Joule*, 2018, **2**, 1573–1594.
35 J. Bao, W. Lu, J. Zhao and X. T. Bi, *Carbon Resour. Convers.*, 2018, **1**, 183–190.
36 R. S. Middleton, G. N. Keating, H. S. Viswanathan, P. H. Stauffer and R. J. Pawar, *Int. J. Greenhouse Gas Control*, 2012, **8**, 132–142.
37 UNCTAD, Journal, 2018.
38 BP Statistical Review of World Energy, https://www.bp.com/en/global/corporate/energy-economics/statistical-review-of-world-energy.html.
39 EIA, Technically Recoverable Shale Oil and Shale Gas Resources, https://www.eia.gov/analysis/studies/worldshalegas/.
40 EIA, Journal, 2019, 2019-010-01.
41 R. S. Middleton, R. Gupta, J. D. Hyman and H. S. Viswanathan, *Appl. Energy*, 2017, **199**, 88–95.
42 D. Malakoff, *Science*, 2014, **344**, 1464–1467.
43 M. Thomas, N. Pidgeon, D. Evensen, T. Partridge, A. Hasell, C. Enders, B. Herr Harthorn and M. Bradshaw, *Wiley Interdiscip. Rev. Clim. Change*, 2017, **8**, e450.
44 W. A. M. Wanniarachchi, P. G. Ranjith and M. S. A. Perera, *Environ. Earth Sci.*, 2017, **76**, 91.
45 L. Wang, Y. Tian, X. Yu, C. Wang, B. Yao, S. Wang, P. H. Winterfeld, X. Wang, Z. Yang, Y. Wang, J. Cui and Y.-S. Wu, *Fuel*, 2017, **210**, 425–445.

46 B. Hou, R. Zhang, Y. Zeng, W. Fu, Y. Muhadasi and M. Chen, *J. Pet. Sci. Eng.*, 2018, **170**, 231–243.
47 Z. Zhou, H. Abass, X. Li and T. Teklu, *J. Nat. Gas Sci. Eng.*, 2016, **29**, 413–430.
48 P. Tan, Y. Jin, K. Han, B. Hou, M. Chen, X. Guo and J. Gao, *Fuel*, 2017, **206**, 482–493.
49 W. A. M. Wanniarachchi, P. G. Ranjith, M. S. A. Perera, T. D. Rathnaweera, D. C. Zhang and C. Zhang, *Eng. Fract. Mech.*, 2018, **194**, 117–135.
50 A. Kotsakis, *Rev. Eur. Community Int. Environ. Law*, 2012, **21**, 282–290.
51 S. Bilgen and İ. Sarıkaya, *J. Nat. Gas Sci. Eng.*, 2016, **35**, 637–645.
52 T. G. Burton, H. S. Rifai, Z. L. Hildenbrand, D. D. Carlton, B. E. Fontenot and K. A. Schug, *Sci. Total Environ*, 2016, **545-546**, 114–126.
53 M. Vishkai and I. Gates, *J. Pet. Sci. Eng.*, 2019, **174**, 1127–1141.
54 Z. Lian, H. Yu, T. Lin and J. Guo, *J. Nat. Gas Sci. Eng.*, 2015, **23**, 538–546.
55 L. Gandossi, Eur. Commisison Jt. Res. Cent. Tech. Reports, 2013, **26347**.
56 F. Gao, C. Cai and Y. Yang, *Results Phys.*, 2018, **9**, 252–262.
57 R. Myers, presented in part at the SPE/AAPG Eastern Regional Meeting, Pittsburgh, Pennsylvania, USA, 2018/10/5/, 2018.
58 W. A. M. Wanniarachchi, P. G. Ranjith, M. S. A. Perera, A. Lashin, N. Al Arifi and J. C. Li, *Geomech. Geophys. Geo-Energy Geo-Resources*, 2015, **1**, 121–134.
59 Z. Jing, C. Feng, S. Wang, D. Xu and G. Xu, *J. Pet. Sci. Eng.*, 2017, **159**, 710–716.
60 G. Beck, C. Nolen, K. Hoopes, C. Krouse, M. Poerner, A. Phatak and S. Verma, presented in part at the SPE Annual Technical Conference and Exhibition, San Antonio, Texas, USA, 2017/10/9/, 2017.
61 X. Zhao, B. Huang and J. Xu, *Fuel*, 2019, **236**, 1496–1504.
62 P. Hou, F. Gao, Y. Gao, Y. Yang and C. Cai, *Int. J. Rock Mech. Min. Sci.*, 2018, **109**, 84–90.
63 C. T. Montgomery and M. B. Smith, *J. Pet. Technol.*, 2010, **62**, 26–40.
64 B. Yuan and D. A. Wood, *Fuel*, 2018, **227**, 99–110.
65 R. M. Buono, B. Mayor and E. López-Gunn, *Environ. Sci. Policy*, 2018, **90**, 193–200.
66 J. L. Luek and M. Gonsior, *Water Res.*, 2017, **123**, 536–548.
67 A. Kondash and A. Vengosh, *Environ. Sci. Technol. Lett.*, 2015, **2**, 276–280.
68 D. Jolly, *The New York Times*, 2013, vol. 11.
69 R. E. Blauer and C. A. Kohlhaas, presented in part at the Fall Meeting of the Society of Petroleum Engineers of AIME, Houston, Texas, 1974/1/1/, 1974.
70 X. Kong, J. McAndrew and P. Cisternas, presented in part at the Abu Dhabi International Petroleum Exhibition & Conference, Abu Dhabi, UAE, 2016/11/7/, 2016.
71 L. H. Burke, G. W. Nevison and W. E. Peters, presented in part at the SPE Eastern Regional Meeting, Columbus, Ohio, USA, 2011/1/1/, 2011.
72 M. M. Reynolds, R. C. Bachman and W. E. Peters, presented in part at the SPE Hydraulic Fracturing Technology Conference, The Woodlands, Texas, USA, 2014/2/4/, 2014.
73 X. Sun, X. Liang, S. Wang and Y. Lu, *J. Pet. Sci. Eng.*, 2014, **119**, 104–111.
74 Y. Chen, T. L. Pope and J. C. Lee, presented in part at the SPE European Formation Damage Conference, Sheveningen, The Netherlands, 2005/1/1/, 2005.
75 A. Verma, G. Chauhan and K. Ojha, *Asia-Pac. J. Chem. Eng.*, 2017, **12**, 872–883.
76 S. A. Faroughi, A. J.-C. J. Pruvot and J. McAndrew, *J. Pet. Sci. Eng.*, 2018, **163**, 243–263.
77 Y. Zhang, J. He, X. Li and C. Lin, *J. Pet. Sci. Eng.*, 2019, **173**, 932–940.
78 D. Zhou, G. Zhang, M. Prasad and P. Wang, *Fuel*, 2019, **247**, 126–134.
79 L. Wang, B. Yao, M. Cha, N. B. Alqahtani, T. W. Patterson, T. J. Kneafsey, J. L. Miskimins, X. Yin and Y.-S. Wu, *J. Nat. Gas Sci. Eng.*, 2016, **35**, 160–174.
80 T. Ishida, K. Aoyagi, T. Niwa, Y. Chen, S. Murata, Q. Chen and Y. Nakayama, *Geophys. Res. Lett.*, 2012, **39**, 1–6.
81 A. Rogala, M. Bernaciak, J. Krzysiek and H. Jan, *Physicochem. Probl. Miner. Process.*, 2012, **49**, 313–322.
82 M. D. Zoback and D. J. Arent, *Elements*, 2014, **10**, 251–253.
83 M. Zoback, S. Kitasei and B. Copithorne, *Addressing the environmental risks from shale gas development*, Worldwatch Institute, Washington, DC, 2010.
84 A. Vengosh, N. Warner, R. Jackson and T. Darrah, *Procedia Earth Planet. Sci.*, 2013, **7**, 863–866.
85 U. S. EPA, Hydraulic Fracturing for Oil and Gas: Impacts from the Hydraulic Fracturing Water Cycle on Drinking Water Resources in the United States.
86 D. Zhang and T. Yang, *Pet. Explor. Dev.*, 2015, **42**, 876–883.
87 J. Currie, M. Greenstone and K. Meckel, *Sci. Adv.*, 2017, **3**, e1603021.
88 D. Kaden and T. Rose, *Environmental and health issues in unconventional oil and gas development*, Elsevier, Amsterdam, Boston, 2016.
89 M. Schimmel, W. Liu and E. Worrell, *Earth-Sci. Rev.*, 2019, **194**, 455–471.
90 D. Elsworth, C. J. Spiers and A. R. Niemeijer, *Science*, 2016, **354**, 1380.
91 U. S. EPA, U.S. Environmental Protection Agency, 2015, EPA/600/R-615/047.
92 R. D. Vidic, S. L. Brantley, J. M. Vandenbossche, D. Yoxtheimer and J. D. Abad, *Science*, 2013, **340**, 1235009.
93 N. R. Warner, R. B. Jackson, T. H. Darrah, S. G. Osborn, A. Down, K. Zhao, A. White and A. Vengosh, *Proc. Natl. Acad. Sci. U. S. A.*, 2012, **109**, 11961–11966.
94 T. Engelder, *Proc. Natl. Acad. Sci. U. S. A.*, 2012, **109**, E3625.
95 G. T. Llewellyn, F. Dorman, J. L. Westland, D. Yoxtheimer, P. Grieve, T. Sowers, E. Humston-Fulmer and S. L. Brantley, *Proc. Natl. Acad. Sci. U. S. A.*, 2015, **112**, 6325–6330.
96 P. A. Hammond, T. Wen, S. L. Brantley and T. Engelder, *Hydrogeol. J.*, 2020, **28**, 1481–1502.

97 R. D. Vidic, S. L. Brantley, J. M. Vandenbossche, D. Yoxtheimer and J. D. Abad, *Science*, 2013, **340**, 1235009.
98 S. G. Osborn, A. Vengosh, N. R. Warner and R. B. Jackson, *Proc. Natl. Acad. Sci. U. S. A.*, 2011, **108**, 8172.
99 M. A. Q. Siddiqui, S. Ali, H. Fei and H. Roshan, *Earth-Sci. Rev.*, 2018, **181**, 1–11.
100 Z. Gao, Y. Fan, Q. Hu, Z. Jiang, Y. Cheng and Q. Xuan, *Mar. Pet. Geol.*, 2019, **109**, 330–338.
101 P. Mohammadmoradi and A. Kantzas, *Can. J. Chem. Eng.*, 2019, **97**, 1627–1642.
102 Y. Shen, H. Ge, M. Meng, Z. Jiang and X. Yang, *Energy Fuels*, 2017, **31**, 4973–4980.
103 T. Liang, X. Luo, Q. Nguyen and D. A. DiCarlo, *Spe J.*, 2018, **23**, 762–771.
104 T. Liang, F. Zhou, J. Lu, D. DiCarlo and Q. Nguyen, *Fuel*, 2017, **209**, 650–660.
105 Y. Shen, H. Ge, C. Li, X. Yang, K. Ren, Z. Yang and S. Su, *J. Nat. Gas Sci. Eng.*, 2016, **35**, 1121–1128.
106 A. Zolfaghari, H. Dehghanpour and J. Holyk, *Int. J. Coal Geol.*, 2017, **179**, 130–138.
107 A. Skempton, *Selected Papers on Soil Mechanics*, 1953, 106–118.
108 A. A. Sabtan, *J. Asian Earth Sci.*, 2005, **25**, 747–757.
109 A. O. Erol and A. Dhowian, *Q. J. Eng. Geol. Hydrogeol.*, 1990, **23**, 243–254.
110 Z. Abiddin Erguler and R. Ulusay, *Eng. Geol.*, 2003, **67**, 331–352.
111 L. t. Johnson and D. Snethen, *ASTM Geotech. Test. J.*, 1978, **1**, 1–8.
112 Q. Lyu, P. Ranjith, X. Long, Y. Kang and M. Huang, *J. Nat. Gas Sci. Eng.*, 2015, **27**, 1421–1431.
113 D. Feng, X. Li, X. Wang, J. Li, F. Sun, Z. Sun, T. Zhang, P. Li, Y. Chen and X. Zhang, *Appl. Clay Sci.*, 2018, **155**, 126–138.
114 R. A. Longoria, T. Liang, U. T. Huynh, Q. P. Nguyen and D. A. DiCarlo, *Spe J.*, 2017, **22**, 1393–1401.
115 BP, Statistical Review of World Energy, https://www.bp.com/content/dam/bp/business-sites/en/global/corporate/pdfs/energy-economics/statistical-review/bp-stats-review-2019-full-report.pdf.
116 Global CO2 emissions in 2019, https://www.iea.org/articles/global-co2-emissions-in-2019.
117 M. M. F. Hasan, E. L. First, F. Boukouvala and C. A. Floudas, *Comput. Chem. Eng.*, 2015, **81**, 2–21.
118 T. Skodvin and K. H. Alfsen, *The Intergovernmental Panel on Climate Change (IPCC): Outline of an assessment*, 2010.
119 P. Markewitz, W. Kuckshinrichs, W. Leitner, J. Linssen, P. Zapp, R. Bongartz, A. Schreiber and T. E. Müller, *Energy Environ. Sci.*, 2012, **5**, 7281–7305.
120 G. P. Peters, G. Marland, C. Le Quéré, T. Boden, J. G. Canadell and M. R. Raupach, *Nat. Clim. Change*, 2012, **2**, 2–4.
121 R. Afroz, M. N. Hassan and N. A. Ibrahim, *Environ. Res.*, 2003, **92**, 71–77.
122 T. H. Oh, *Renewable Sustainable Energy Rev.*, 2010, **14**, 2697–2709.
123 Scripps CO2 Program: CO2 concentration at Mauna Loa Observatory, Hawaii, http://scrippsco2.ucsd.edu.
124 R. M. Cuéllar-Franca and A. Azapagic, *J. CO2 Util.*, 2015, **9**, 82–102.
125 Z. Dai, R. Middleton, H. Viswanathan, J. Fessenden-Rahn, J. Bauman, R. Pawar, S.-Y. Lee and B. McPherson, *Environ. Sci. Technol. Lett.*, 2014, **1**, 49–54.
126 M. Aresta, *Utilization of Dense Carbon Dioxide as an Inert Solvent for Chemical Syntheses*, Wiley-VCH, 2010.
127 E. Alper and O. Yuksel Orhan, *Petroleum*, 2017, **3**, 109–126.
128 H. B. Jung, K. C. Carroll, S. Kabilan, D. J. Heldebrant, D. Hoyt, L. Zhong, T. Varga, S. Stephens, L. Adams, A. Bonneville, A. Kuprat and C. A. Fernandez, *Green Chem.*, 2015, **17**, 2799–2812.
129 R. S. Norhasyima and T. M. I. Mahlia, *J. CO2 Util.*, 2018, **26**, 323–335.
130 F. I. Stalkup Jr, *J. Pet. Technol.*, 1983, **35**, 815–826.
131 J. J. Sheng, *J. Pet. Sci. Eng.*, 2017, **159**, 654–665.
132 M. K. Verma, *Fundamentals of carbon dioxide-enhanced oil recovery (CO2-EOR): a supporting document of the assessment methodology for hydrocarbon recovery using CO2-EOR associated with carbon sequestration*, 2015.
133 J. Davidson, P. Freund and A. Smith, *Putting Carbon Back in the Ground*, IEA, 2001.
134 S. Bachu, *Energy Convers. Manage.*, 2000, **41**, 953–970.
135 M. Salehpour, M. Riazi, M. R. Malayeri and M. Seyyedi, *J. Pet. Sci. Eng.*, 2020, **195**, 107663.
136 V. A. Kuuskraa and T. Malone, presented in part at the Offshore Technology Conference, Houston, Texas, USA, 2016/5/2/, 2016.
137 B. Chen and R. Pawar, presented in part at the SPE Annual Technical Conference and Exhibition, Dallas, Texas, USA, 2018/9/24/, 2018.
138 D. Merchant, presented in part at the Carbon Management Technology Conference, Houston, Texas, USA, 2019/11/13/, 2019.
139 A. Hemmati-Sarapardeh, S. Ayatollahi, M.-H. Ghazanfari and M. Masihi, *J. Chem. Eng. Data*, 2014, **59**, 61–69.
140 M. Lashkarbolooki and S. Ayatollahi, *Chin. J. Chem. Eng.*, 2018, **26**, 373–379.
141 Z. Song, Y. Song, Y. Li, B. Bai, K. Song and J. Hou, *Fuel*, 2020, **276**, 118006.
142 Carbon Capture, Use, and Storage (CCUS) Report, National Petroleum Council, U.S., 2019.
143 M. Bui, C. S. Adjiman, A. Bardow, E. J. Anthony, A. Boston, S. Brown, P. S. Fennell, S. Fuss, A. Galindo, L. A. Hackett, J. P. Hallett, H. J. Herzog, G. Jackson, J. Kemper, S. Krevor, G. C. Maitland, M. Matuszewski, I. S. Metcalfe, C. Petit, G. Puxty, J. Reimer, D. M. Reiner, E. S. Rubin, S. A. Scott, N. Shah, B. Smit, J. P. M. Trusler, P. Webley, J. Wilcox and N. Mac Dowell, *Energy Environ. Sci.*, 2018, **11**, 1062–1176.
144 EIA, U.S. Coalbed Methane Proved Reserves, https://www.eia.gov/dnav/ng/ng_enr_coalbed_a_EPG0_R51_Bcf_a.htm.
145 M. Mukherjee and S. Misra, *Earth-Sci. Rev.*, 2018, **179**, 392–410.
146 R. Sander, L. D. Connell, Z. Pan, M. Camilleri, D. Heryanto and N. Lupton, *Int. J. Coal Geol.*, 2014, **131**, 113–125.
147 W. B. Fei, Q. Li, X. C. Wei, R. R. Song, M. Jing and X. C. Li, *Eng. Geol.*, 2015, **196**, 194–209.

148 G. J. Koperna and D. E. Riestenberg, presented in part at the SPE International Conference on CO2 Capture, Storage, and Utilization, San Diego, California, USA, 2009/1/1/, 2009.
149 C. Temizel, D. J. Betancourt, A. Tiwari, M. Zhang, S. S. Aktas and F. Quiros, presented in part at the SPE Argentina Exploration and Production of Unconventional Resources Symposium, Buenos Aires, Argentina, 2016/6/1/, 2016.
150 M. Mazzotti, R. Pini and G. Storti, *J. Supercrit. Fluids*, 2009, **47**, 619–627.
151 A. Busch and Y. Gensterblum, *Int. J. Coal Geol.*, 2011, **87**, 49–71.
152 O. Ola, M. Mercedes Maroto-Valer and S. Mackintosh, *Energy Procedia*, 2013, **37**, 6704–6709.
153 F. D. Meylan, V. Moreau and S. Erkman, *J. CO2 Util.*, 2015, **12**, 101–108.
154 A. Dibenedetto, A. Angelini and P. Stufano, *J. Chem. Technol. Biotechnol.*, 2014, **89**, 334–353.
155 A. A. Olajire, *J. Pet. Sci. Eng.*, 2013, **109**, 364–392.
156 S. J. Gerdemann, W. K. O'Connor, D. C. Dahlin, L. R. Penner and H. Rush, *Environ. Sci. Technol.*, 2007, **41**, 2587–2593.
157 S.-Y. Pan, P.-C. Chiang, W. Pan and H. Kim, *Crit. Rev. Environ. Sci. Technol.*, 2018, **48**, 471–534.
158 E. Georgakopoulos, R. M. Santos, Y. W. Chiang and V. Manovic, *Greenhouse Gases: Sci. Technol.*, 2016, **6**, 470–491.
159 S.-L. Pei, S.-Y. Pan, Y.-M. Li and P.-C. Chiang, *Environ. Sci. Technol.*, 2017, **51**, 10674–10681.
160 H. Xie, H. Yue, J. Zhu, B. Liang, C. Li, Y. Wang, L. Xie and X. Zhou, *Engineering*, 2015, **1**, 150–157.
161 A. F. Esteves, F. M. Santos and J. C. Magalhães Pires, *Renewable Sustainable Energy Rev.*, 2019, **114**, 109331.
162 C. Pan, O. Chávez, C. E. Romero, E. K. Levy, A. Aguilar Corona and C. Rubio-Maya, *Energy*, 2016, **102**, 148–160.
163 C. Xu, P. Dowd and Q. Li, *J. Rock Mech. Geotech. Eng.*, 2016, **8**, 50–59.
164 H. Shao, S. Kabilan, S. Stephens, N. Suresh, A. N. Beck, T. Varga, P. F. Martin, A. Kuprat, H. B. Jung, W. Um, A. Bonneville, D. J. Heldebrant, K. C. Carroll, J. Moore and C. A. Fernandez, *Geothermics*, 2015, **58**, 22–31.
165 C. A. Fernandez, V. Gupta, G. L. Dai, A. P. Kuprat, A. Bonneville, D. Appriou, J. A. Horner, P. F. Martin and J. A. Burghardt, *ACS Sustainable Chem. Eng.*, 2019, **7**, 19660–19668.
166 D. Chiaramonti, M. Prussi, D. Casini, M. R. Tredici, L. Rodolfi, N. Bassi, G. C. Zittelli and P. Bondioli, *Appl. Energy*, 2013, **102**, 101–111.
167 E. Sadatshojaei, D. A. Wood and D. Mowla, in *Sustainable Green Chemical Processes and their Allied Applications*, ed. Inamuddin and A. Asiri, Springer International Publishing, Cham, 2020, pp. 575–588, DOI: 10.1007/978-3-030-42284-4_21.
168 J. D. Figueroa, T. Fout, S. Plasynski, H. McIlvried and R. D. Srivastava, *Int. J. Greenhouse Gas Control*, 2008, **2**, 9–20.
169 R. S. Middleton, G. N. Keating, P. H. Stauffer, A. B. Jordan, H. S. Viswanathan, Q. J. Kang, J. W. Carey, M. L. Mulkey, E. J. Sullivan, S. P. Chu, R. Esposito and T. A. Meckel, *Energy Environ. Sci.*, 2012, **5**, 7328–7345.
170 Developments and Innovation in Carbon Dioxide (CO_2) Capture and Storage Technology: Carbon Dioxide (CO_2) Storage and Utilisation, Elsevier, 2010.
171 B. P. McGrail, H. T. Schaef, V. A. Glezakou, L. X. Dang and A. T. Owen, *Energy Procedia*, 2009, **1**, 3415–3419.
172 M. E. Boot-Handford, J. C. Abanades, E. J. Anthony, M. J. Blunt, S. Brandani, N. Mac Dowell, J. R. Fernández, M.-C. Ferrari, R. Gross, J. P. Hallett, R. S. Haszeldine, P. Heptonstall, A. Lyngfelt, Z. Makuch, E. Mangano, R. T. J. Porter, M. Pourkashanian, G. T. Rochelle, N. Shah, J. G. Yao and P. S. Fennell, *Energy Environ. Sci.*, 2014, **7**, 130–189.
173 K. S. Lackner, *Science*, 2003, **300**, 1677.
174 Z. Li, M. Dong, S. Li and S. Huang, *Energy Convers. Manage.*, 2006, **47**, 1372–1382.
175 H. T. Schaef, C. L. Davidson, A. T. Owen, Q. R. S. Miller, J. S. Loring, C. J. Thompson, D. H. Bacon, V. A. Glezakou and B. P. McGrail, *Energy Procedia*, 2014, **63**, 7844–7851.
176 Y. W. Liwei Zhang, X. Miao, M. Gan and X. Li, *Adv. Geo-Energy Res.*, 2019, **3**, 304–313.
177 C. D. Wallace, R. Ershadnia and M. R. Soltanian, *Adv. Geo-Energy Res.*, 2020, **4**, 392–405.
178 D. A. Voormeij and G. J. Simandl, *Geoscience Canada*, 2004, **31**, 265–275.
179 L. G. H. van der Meer, in *Greenhouse Gas Control Technologies - 6th International Conference*, ed. J. Gale and Y. Kaya, Pergamon, Oxford, 2003, pp. 201–206, DOI: 10.1016/B978-008044276-1/50032-5.
180 Carbon Capture, Use, and Storage (CCUS) Report, National Petroleum Council, U.S., 2019.
181 ISO, *Journal*, 2019, 27916:2019.
182 S. M. Benson and J. Deutch, *Joule*, 2018, **2**, 1386–1389.
183 R. S. Middleton, B. Chen, D. R. Harp, R. M. Kammer, J. D. Ogland-Hand, J. M. Bielicki, A. F. Clarens, R. P. Currier, K. M. Ellett, B. A. Hoover, D. N. McFarlane, R. J. Pawar, P. H. Stauffer, H. S. Viswanathan and S. P. Yaw, *Appl. Comput. Geosci.*, 2020, **7**, 100035.
184 R. S. Middleton, J. D. Ogland-Hand, B. Chen, J. M. Bielicki, K. M. Ellett, D. R. Harp and R. M. Kammer, *Energy Environ. Sci.*, 2020, **13**, 5000–5016.
185 Y. Lu, J. Tang, Z. Ge, B. Xia and Y. Liu, *Int. J. Rock Mech. Min. Sci.*, 2013, **60**, 47–56.
186 K. Peng, S. Tian, G. Li, Z. Huang, R. Yang and Z. Guo, *Pet. Explor. Dev.*, 2018, **45**, 343–350.
187 R. Wang, W. Zhou, Z. Shen and Y. Yang, *China Safety Science Journal*, 1999, **9**, 1–5.
188 X. Li, Z. Feng, G. Han, D. Elsworth, C. Marone, D. Saffer and D. S. Cheon, *Geomech. Geophys. Geo-Energy Geo-Resources*, 2016, **2**, 63–76.
189 J. J. Kolle, *CIM International Conference on Horizontal Well Technology*, Calgary, Alberta, Canada, 2000.
190 S. Tian, Z. He, G. Li, H. Wang, Z. Shen and Q. Liu, *J. Nat. Gas Sci. Eng.*, 2016, **29**, 232–242.

191 A. P. Gupta, A. Gupta and J. Langlinais, presented in part at the SPE Annual Technical Conference and Exhibition, Dallas, Texas, 2005/1/1/, 2005.
192 F. A. Al-Adwani, J. Langlinais and R. G. Hughes, *SPE Drill. Completion*, 2009, **24**, 599–610.
193 Y. Du, R. Wang, H. Ni, M. Li, W. Song and H. Song, *J. Hydrodyn., Ser. B*, 2012, **24**, 554–560.
194 Y. Du, R. Wang, H. Ni, Z. Huang and M. Li, *J. Hydrodyn., Ser. B*, 2013, **25**, 528–534.
195 M. Huang, Y. Kang, X. Wang, Y. Hu, D. Li, C. Cai and Y. Liu, *Exp. Therm. Fluid Sci.*, 2018, **94**, 304–315.
196 R. H. Wang, H. J. Huo, Z. Y. Huang, H. F. Song and H. J. Ni, *J. Hydrodyn.*, 2014, **26**, 226–233.
197 Y. Hu, Y. Kang, X. Wang, X. Li, M. Huang and M. Zhang, *J. Nat. Gas Sci. Eng.*, 2016, **36**, 108–116.
198 Z. He, S. Tian, G. Li, H. Wang, Z. Shen and Z. Xu, *J. Nat. Gas Sci. Eng.*, 2015, **27**, 842–851.
199 X. Long, Q. Liu, X. Ruan, Y. Kang and Q. Lyu, *J. Nat. Gas Sci. Eng.*, 2016, **34**, 1044–1053.
200 M. Huang, Y. Kang, X. Wang, Y. Hu, C. Cai, Y. Liu and H. Chen, *Appl. Therm. Eng.*, 2018, **139**, 445–455.
201 X. Sun, H. Ni, R. Wang, Z. Shen and M. Zhao, *J. Pet. Sci. Eng.*, 2018, **162**, 532–538.
202 H. Huo, R. Wang, H. Ni, Y. Li, C. Tan and S. Xue, *J. CO2 Util.*, 2017, **20**, 105–112.
203 R. M. Enick and J. Ammer, *Website of the National Energy Technology Laboratory*, 1998.
204 P. Peng, Y. Ju, Y. Wang, S. Wang and F. Gao, *Int. J. Numer. Anal. Methods*, 2017, **41**, 1992–2013.
205 P. Pei, K. Ling, J. He and Z. Liu, *J. Nat. Gas Sci. Eng.*, 2015, **26**, 1595–1606.
206 T. Ishida, Y. Chen, Z. Bennour, H. Yamashita, S. Inui, Y. Nagaya, M. Naoi, Q. Chen, Y. Nakayama and Y. Nagano, *J. Geophys. Res.: Solid Earth*, 2016, **121**, 8080–8098.
207 X. Zhang, J. G. Wang, F. Gao and Y. Ju, *J. Nat. Gas Sci. Eng.*, 2017, **45**, 291–306.
208 L. Wang, B. Yao, H. Xie, P. H. Winterfeld, T. J. Kneafsey, X. Yin and Y.-S. Wu, *Energy*, 2017, **139**, 1094–1110.
209 J. Wang, D. Elsworth, Y. Wu, J. Liu, W. Zhu and Y. Liu, *Rock Mech. Rock Eng.*, 2018, **51**, 299–313.
210 X. Zhang, Y. Lu, J. Tang, Z. Zhou and Y. Liao, *Fuel*, 2017, **190**, 370–378.
211 L. Liu, W. Zhu, C. Wei, D. Elsworth and J. Wang, *J. Pet. Sci. Eng.*, 2018, **164**, 91–102.
212 J. He, L. O. Afolagboye, C. Lin and X. Wan, *Energies*, 2018, **11**, 557.
213 S. Li and D. Zhang, *Spe J.*, 2019, **24**, 857–876.
214 X. Song, Y. Guo, J. Zhang, N. Sun, G. Shen, X. Chang, W. Yu, Z. Tang, W. Chen, W. Wei, L. Wang, J. Zhou, X. Li, X. Li, J. Zhou and Z. Xue, *Joule*, 2019, **3**, 1913–1926.
215 Y. Jia, Y. Lu, D. Elsworth, Y. Fang and J. Tang, *J. Pet. Sci. Eng.*, 2018, **165**, 284–297.
216 Y. Jiang, C. Qin, Z. Kang, J. Zhou, Y. Li, H. Liu and X. Song, *J. Nat. Gas Sci. Eng.*, 2018, **55**, 382–394.
217 X. Li, G. Li, W. Yu, H. Wang, K. Sepehrnoori, Z. Chen, H. Sun and S. Zhang, in *Unconventional Resources Technology Conference*, Austin, Texas, 24-26 July 2017, Society of Exploration Geophysicists, American Association of Petroleum Geologists, Society of Petroleum Engineers, 2017, pp. 2129–2144, DOI: 10.15530/urtec-2017-2687198.
218 Q. Lv, X. Long, Y. Kang, L. Xiao and W. Wu, presented in part at the 6th International Conference on Pumps and Fans with Compressors and Wind Turbines, Beijing, China, 2013.
219 J. J. Watkins and T. J. McCarthy, *Chem. Mater.*, 1995, **7**, 1991–1994.
220 M. Raje, K. Asghari, S. Vossoughi, D. W. Green and G. P. Willhite, *SPE Reservoir Eval. Eng.*, 1999, **2**, 205–210.
221 C. Shi, Z. Huang, S. Kilic, J. Xu, R. M. Enick, E. J. Beckman, A. J. Carr, R. E. Melendez and A. D. Hamilton, *Science*, 1999, **286**, 1540.
222 A. Choubineh, A. Helalizadeh and D. Awood, *Pet. Sci.*, 2019, 117–126.
223 J. Zhou, N. Hu, X. Xian, L. Zhou, J. Tang, Y. Kang and H. Wang, *Adv. Geo-Energy Res.*, 2019, **3**, 207–224.
224 E. I. Administration and V. Kuuskraa, *World shale gas resources: an initial assessment of 14 regions outside the United States*, US Department of Energy, USA, 2011.
225 S. M. Benson, P. Cook, J. Anderson, S. H. Bachu, B. Nimir, B. Basu, J. Bradshaw, G. Deguchi, J. Gale and G. von-Goerne, *Underground Geological Storage*, Cambridge, England, 2005.
226 A. Busch, S. Alles, Y. Gensterblum, D. Prinz, D. N. Dewhurst, M. D. Raven, H. Stanjek and B. M. Krooss, *Int. J. Greenhouse Gas Control*, 2008, **2**, 297–308.
227 S. M. Kang, E. Fathi, R. J. Ambrose, I. Y. Akkutlu and R. F. Sigal, *Spe J.*, 2011, **16**, 842–855.
228 F. Liu, K. Ellett, Y. Xiao and J. A. Rupp, *Int. J. Greenhouse Gas Control*, 2013, **17**, 111–126.
229 B. Hazra, D. A. Wood, V. Vishal and A. K. Singh, *Energy Fuels*, 2018, **32**, 8175–8186.
230 S. J. Altman, B. Aminzadeh, M. T. Balhoff, P. C. Bennett, S. L. Bryant, M. B. Cardenas, K. Chaudhary, R. T. Cygan, W. Deng, T. Dewers, D. A. DiCarlo, P. Eichhubl, M. A. Hesse, C. Huh, E. N. Matteo, Y. Mehmani, C. M. Tenney and H. Yoon, *J. Phys. Chem. C*, 2014, **118**, 15103–15113.
231 I. Okamoto, X. Li and T. Ohsumi, *Energy*, 2005, **30**, 2344–2351.
232 D. B. Bennion and S. Bachu, presented in part at the EUROPEC/EAGE Conference and Exhibition, London, UK, 2007/1/1/, 2007.
233 B. Bennion and S. Bachu, *SPE Reservoir Eval. Eng.*, 2008, **11**, 487–496.
234 F. Civan, *AIP Conf. Proc.*, 2010, **1254**, 53–58.
235 A. Sakhaee-Pour and S. Bryant, *SPE Reservoir Eval. Eng.*, 2012, **15**, 401–409.
236 A. S. Ziarani and R. Aguilera, *Transp. Porous Media*, 2012, **91**, 239–260.
237 W. Shen, L. Zheng, C. M. Oldenburg, A. Cihan, J. Wan and T. K. Tokunaga, *Transp. Porous Media*, 2018, **123**, 521–531.
238 Z. Liehui, S. Baochao, Z. Yulong and G. Zhaoli, *Int. J. Heat Mass Transfer*, 2019, **139**, 144–179.

239 M. Gutierrez, L. E. Øino and R. Nygård, *Mar. Pet. Geol.*, 2000, **17**, 895–907.
240 T. Phillips, N. Kampman, K. Bisdom, N. D. Forbes Inskip, S. A. M. den Hartog, V. Cnudde and A. Busch, *Earth-Sci. Rev.*, 2020, **211**, 103390.
241 R. M. Bustin, A. M. M. Bustin, A. Cui, D. Ross and V. M. Pathi, presented in part at the SPE Shale Gas Production Conference, Fort Worth, Texas, USA, 2008/1/1/, 2008.
242 F. O. Jones and W. W. Owens, *J. Pet. Technol.*, 1980, **32**, 1631–1640.
243 J. Zhang, S. Huang, L. Cheng, W. Xu, H. Liu, Y. Yang and Y. Xue, *J. Nat. Gas Sci. Eng.*, 2015, **24**, 291–301.
244 R. Raghavan and L. Y. Chin, presented in part at the SPE Annual Technical Conference and Exhibition, San Antonio, Texas, 2002/1/1/, 2002.
245 A. F. Gangi, *Int. J. Rock Mech. Min. Sci. Geomech. Abstr.*, 1978, **15**, 249–257.
246 A. Wasaki and I. Y. Akkutlu, *Spe J.*, 2015, **20**, 1384–1396.
247 S. Wang, J. Shi, K. Wang, Z. Sun and Z. Zhao, *Energy Fuels*, 2017, **31**, 13545–13557.
248 I. Palmer and J. Mansoori, presented in part at the SPE Annual Technical Conference and Exhibition, Denver, Colorado, 1996/1/1/, 1996.
249 J. A. Rushing, K. E. Newsham, P. M. Lasswell, J. C. Cox and T. A. Blasingame, presented in part at the SPE Annual Technical Conference and Exhibition, Houston, Texas, 2004/1/1/, 2004.
250 E. Fathi, A. Tinni and I. Y. Akkutlu, *Shale Gas Correction to Klinkenberg Slip Theory*, 2012.
251 D. A. Lockerby, J. M. Reese and M. A. Gallis, *AIAA J.*, 2005, **43**, 1391–1393.
252 L. J. Klinkenberg, presented in part at the Drilling and Production Practice, New York, New York, 1941/1/1/, 1941.
253 R. W. Barber and D. R. Emerson, *Heat Transfer Eng.*, 2006, **27**, 3–12.
254 H. Singh and F. Javadpour, *Fuel*, 2016, **164**, 28–37.
255 J. B. Curtis, *AAPG Bull.*, 2002, **86**, 1921–1938.
256 F. Javadpour, D. Fisher and M. Unsworth, *J. Can. Pet. Technol.*, 2007, **46**, 55–61.
257 R. J. Ambrose, R. C. Hartman, M. Diaz Campos, I. Y. Akkutlu and C. Sondergeld, *SPE unconventional gas conference*, 2010.
258 G. R. Chalmers and R. M. Bustin, *Bull. Can. Pet. Geol.*, 2008, **56**, 22–61.
259 R. J. Hill, E. Zhang, B. J. Katz and Y. Tang, *AAPG Bull.*, 2007, **91**, 501–521.
260 D. J. Ross and R. M. Bustin, *AAPG Bull.*, 2008, **92**, 87–125.
261 D. J. K. Ross and R. Marc Bustin, *Mar. Pet. Geol.*, 2009, **26**, 916–927.
262 M. Gasparik, P. Bertier, Y. Gensterblum, A. Ghanizadeh, B. M. Krooss and R. Littke, *Int. J. Coal Geol.*, 2014, **123**, 34–51.
263 G. R. Chalmers and R. M. Bustin, *Int. J. Coal Geol.*, 2007, **70**, 223–239.
264 S. Wang, Z. Song, T. Cao and X. Song, *Mar. Pet. Geol.*, 2013, **44**, 112–119.
265 J. Tan, P. Weniger, B. Krooss, A. Merkel, B. Horsfield, J. Zhang, C. J. Boreham, G. V. Graas and B. A. Tocher, *Fuel*, 2014, **129**, 204–218.
266 M. M. Dubinin, in *Progress in Surface and Membrane Science*, ed. D. A. Cadenhead, J. F. Danielli and M. D. Rosenberg, Elsevier, 1975, vol. 9, pp. 1–70.
267 A. Miceli Romero and R. P. Philp, *AAPG Bull.*, 2012, **96**, 493–517.
268 T. Zhang, G. S. Ellis, S. C. Ruppel, K. Milliken and R. Yang, *Org. Geochem.*, 2012, **47**, 120–131.
269 X. Lu, F. Li and A. T. Watson, *SPE Form. Eval.*, 1995, **10**, 109–113.
270 M. Gasparik, A. Ghanizadeh, P. Bertier, Y. Gensterblum, S. Bouw and B. M. Krooss, *Energy Fuels*, 2012, **26**, 4995–5004.
271 L. Ji, T. Zhang, K. L. Milliken, J. Qu and X. Zhang, *Appl. Geochem.*, 2012, **27**, 2533–2545.
272 A. Merkel, R. Fink and R. Littke, *Int. J. Coal Geol.*, 2015, **147–148**, 1–8.
273 X. Luo, S. Wang, Z. Wang, Z. Jing, M. Lv, Z. Zhai and T. Han, *Int. J. Coal Geol.*, 2015, **150–151**, 210–223.
274 D. S. Berawala and P. Ø. Andersen, *SPE Reservoir Eval. Eng.*, 2020, 17, preprint.
275 A. Bemani, A. Baghban, A. H. Mohammadi and P. Ø. Andersen, *J. Nat. Gas Sci. Eng.*, 2020, **76**, 103204.
276 I. Klewiah, D. S. Berawala, H. C. Alexander Walker, P. Ø. Andersen and P. H. Nadeau, *J. Nat. Gas Sci. Eng.*, 2020, **73**, 103045.
277 B. C. Nuttal, C. Eble, R. M. Bustin and J. A. Drahovzal, in *Greenhouse Gas Control Technologies 7*, ed. E. S. Rubin, D. W. Keith, C. F. Gilboy, M. Wilson, T. Morris, J. Gale and K. Thambimuthu, Elsevier Science Ltd, Oxford, 2005, pp. 2225–2228, DOI: 10.1016/B978-008044704-9/50306-2.
278 P. Weniger, W. Kalkreuth, A. Busch and B. M. Krooss, *Int. J. Coal Geol.*, 2010, **84**, 190–205.
279 S. Duan, M. Gu, X. Du and X. Xian, *Energy Fuels*, 2016, **30**, 2248–2256.
280 J. Zhou, S. Xie, Y. Jiang, X. Xian, Q. Liu, Z. Lu and Q. Lyu, *Energy Fuels*, 2018, **32**, 6073–6089.
281 J. Liu, L. Xie, D. Elsworth and Q. Gan, *Environ. Sci. Technol.*, 2019, **53**, 9328–9336.
282 Y. Wang, T. T. Tsotsis and K. Jessen, *Ind. Eng. Chem. Res.*, 2015, **54**, 12187–12195.
283 M. Gu, X. Xian, S. Duan and X. Du, *J. Nat. Gas Sci. Eng.*, 2017, **46**, 296–306.
284 T. Wang, S. Tian, G. Li and M. Sheng, *J. Nat. Gas Sci. Eng.*, 2018, **50**, 181–188.
285 X.-D. Du, M. Gu, S. Duan and X.-F. Xian, *J. Energy Resour. Technol.*, 2016, **139**, 1–9.
286 Y. Ma, C. Yue, S. Li, X. Xu and Y. Niu, *Carbon Resour. Convers.*, 2019, **2**, 35–42.
287 B. Liu, C. Qi, T. Mai, J. Zhang, K. Zhan, Z. Zhang and J. He, *J. Nat. Gas Sci. Eng.*, 2018, **53**, 329–336.
288 W. Zhou, H. Wang, Y. Yan and X. Liu, *Energy Fuels*, 2019, **33**, 6542–6551.
289 M.-S. Lee, B. P. McGrail, R. Rousseau and V.-A. Glezakou, *J. Phys. Chem. C*, 2018, **122**, 1125–1134.

290 D. Pines, J. Ditkovich, T. Mukra, Y. Miller, P. M. Kiefer, S. Daschakraborty, J. T. Hynes and E. Pines, *J. Phys. Chem. B*, 2016, **120**, 2440–2451.
291 A. Stirling and I. Pápai, *J. Phys. Chem. B*, 2010, **114**, 16854–16859.
292 K. Adamczyk, M. Prémont-Schwarz, D. Pines, E. Pines and E. T. J. Nibbering, *Science*, 2009, **326**, 1690.
293 D. Polino, E. Grifoni, R. Rousseau, M. Parrinello and V.-A. Glezakou, *J. Phys. Chem. A*, 2020, **124**, 3963–3975.
294 T. Loerting and J. Bernard, *ChemPhysChem*, 2010, **11**, 2305–2309.
295 M. T. Nguyen, M. H. Matus, V. E. Jackson, V. T. Ngan, J. R. Rustad and D. A. Dixon, *J. Phys. Chem. A*, 2008, **112**, 10386–10398.
296 N. R. Jena and P. C. Mishra, *Theor. Chem. Acc.*, 2005, **114**, 189–199.
297 P. P. Kumar, A. G. Kalinichev and R. J. Kirkpatrick, *J. Chem. Phys.*, 2007, **126**, 204315.
298 V.-A. Glezakou, R. Rousseau, L. X. Dang and B. P. McGrail, *Phys. Chem. Chem. Phys.*, 2010, **12**, 8759–8771.
299 M. Saharay and S. Balasubramanian, *J. Phys. Chem. B*, 2007, **111**, 387–392.
300 I. Gaus, *Int. J. Greenhouse Gas Control*, 2010, **4**, 73–89.
301 S. Farquhar, J. Pearce, G. Dawson, A. Golab, S. Sommacal, D. Kirste, D. Biddle and S. Golding, *Chem. Geol.*, 2015, **399**, 98–122.
302 M. Watson, *CO_2CRC Publication Number RPT06-0098*, 2006.
303 B. L. Alemu, P. Aagaard, I. A. Munz and E. Skurtveit, *Appl. Geochem.*, 2011, **26**, 1975–1989.
304 J. Zhou, K. Yang, S. Tian, L. Zhou, X. Xian, Y. Jiang, M. Liu and J. Cai, *Fuel*, 2020, **263**, 116642.
305 F. K. Crundwell, *Hydrometallurgy*, 2014, **149**, 265–275.
306 Q. Lyu, X. Long, P. G. Ranjith, J. Tan, Y. Kang and Z. Wang, *Energy*, 2018, **147**, 1288–1298.
307 Q. Lyu, P. Ranjith, X. Long and B. Ji, *Materials*, 2016, **9**, 663.
308 Q. Lyu, X. Long, P. G. Ranjith, J. Tan, J. Zhou, Z. Wang and W. Luo, *Geomech. Geophys. Geo-Energy Geo-Resources*, 2018, **4**, 141–156.
309 H. Yin, J. Zhou, X. Xian, Y. Jiang, Z. Lu, J. Tan and G. Liu, *Energy*, 2017, **132**, 84–95.
310 S. Zhang, X. Xian, J. Zhou and L. Zhang, *RSC Adv.*, 2017, **7**, 42946–42955.
311 G. Feng, Y. Kang, Z.-D. Sun, X.-C. Wang and Y.-Q. Hu, *Energy*, 2019, **173**, 870–882.
312 Y. Zou, S. Li, X. Ma, S. Zhang, N. Li and M. Chen, *J. Nat. Gas Sci. Eng.*, 2018, **49**, 157–168.
313 K. L. Toews, R. M. Shroll, C. M. Wai and N. G. Smart, *Anal. Chem.*, 1995, **67**, 4040–4043.
314 Q. Lyu, J. Tan, J. M. Dick, Q. Liu, R. Pathegama Gamage, L. Li, Z. Wang and C. Hu, *Rock Mech. Rock Eng.*, 2018, **52**, 2039–2052.
315 A. G. Ilgen, M. Aman, D. N. Espinoza, M. A. Rodriguez, J. M. Griego, T. A. Dewers, J. D. Feldman, T. A. Stewart, R. C. Choens and J. Wilson, *Int. J. Greenhouse Gas Control*, 2018, **78**, 244–253.
316 C. K. Ho and S. W. Webb, *Gas Transport in Porous Media*, Springer, Netherlands, 2006.
317 P. Billemont, B. Coasne and G. De Weireld, *Langmuir*, 2013, **29**, 3328–3338.
318 E. Fathi and I. Y. Akkutlu, *Int. J. Coal Geol.*, 2014, **123**, 52–61.
319 X. Li, J. Fan, H. Yu, Y. Zhu and H. Wu, *Int. J. Heat Mass Transfer*, 2018, **122**, 1210–1221.
320 Y. Lan, Z. Yang, P. Wang, Y. Yan, L. Zhang and J. Ran, *Fuel*, 2019, **238**, 412–424.
321 Q. Lyu, K. Wang, W. A. M. Wanniarachchi, C. Hu and J. Shi, *Geomech. Geophys. Geo-Energy Geo-Resources*, 2020, **6**, 69.
322 T. H. Kim, J. Cho and K. S. Lee, *Appl. Energy*, 2017, **190**, 1195–1206.
323 J. Zhou, G. Liu, Y. Jiang, X. Xian, Q. Liu, D. Zhang and J. Tan, *J. Nat. Gas Sci. Eng.*, 2016, **36**, 369–377.
324 W. Wu, M. D. Zoback and A. H. Kohli, *Fuel*, 2017, **203**, 179–186.
325 A. H. Hosseini, H. Ghadery-Fahliyany, D. Wood and A. Choubineh, *Gas Process. J.*, 2020, **8**, 83–92.
326 H. Zhu, Y. Ju, C. Huang, K. Han, Y. Qi, M. Shi, K. Yu, H. Feng, W. Li, L. Ju and J. Qian, *Fuel*, 2019, **241**, 914–932.
327 Y. Ju, C. Huang, Y. Sun, Q. Wan, X. Lu, S. Lu, H. He, X. Wang, C. Zou, J. Wu, H. Liu, L. Shao, X. Wu, H. Chao, Q. Liu, J. Qiu, M. Wang, J. Cai, G. Wang and Y. Sun, *J. Nanosci. Nanotechnol.*, 2017, **17**, 5930–5965.
328 Y. Jiang, Y. Luo, Y. Lu, C. Qin and H. Liu, *Energy*, 2016, **97**, 173–181.
329 Y. Pan, D. Hui, P. Luo, Y. Zhang, L. Zhang and L. Sun, *J. CO_2 Util.*, 2018, **28**, 152–167.
330 K. M. Mouzakis, A. K. Navarre-Sitchler, G. Rother, J. L. Bañuelos, X. Wang, J. P. Kaszuba, J. E. Heath, Q. R. S. Miller, V. Alvarado and J. E. McCray, *Environ. Eng. Sci.*, 2016, **33**, 725–735.
331 J. P. Kaszuba, D. R. Janecky and M. G. Snow, *Chem. Geol.*, 2005, **217**, 277–293.
332 S. Carroll, W. McNab, S. Torres, M. Singleton and P. Zhao, *Energy Procedia*, 2011, **4**, 5186–5194.
333 H. Yin, J. Zhou, Y. Jiang, X. Xian and Q. Liu, *Fuel*, 2016, **184**, 289–303.
334 K. Goto, K. Yogo and T. Higashii, *Appl. Energy*, 2013, **111**, 710–720.
335 A. B. Rao and E. S. Rubin, *Environ. Sci. Technol.*, 2002, **36**, 4467–4475.
336 O. Yevtushenko, D. Bettge, R. Bäßler and S. Bohraus, *Mater. Corros.*, 2015, **66**, 334–341.
337 O. Bolland and H. Undrum, *Adv. Environ. Res.*, 2003, **7**, 901–911.
338 M. Lucquiaud and J. Gibbins, *Chem. Eng. Res. Des.*, 2011, **89**, 1553–1571.
339 A. K. Datta and P. K. Sen, *J. Membr. Sci.*, 2006, **283**, 291–300.
340 F. Ahmad, K. K. Lau, A. M. Shariff and G. Murshid, *Comput. Chem. Eng.*, 2012, **36**, 119–128.
341 R. W. Baker, *Membrane Technology and Applications*, John Wiley & Sons, Chichester, UK, 2nd edn, 2004.
342 J. Hao, P. A. Rice and S. A. Stern, *J. Membr. Sci.*, 2008, **320**, 108–122.

343 B. Jia, J.-S. Tsau and R. Barati, *Fuel*, 2019, **236**, 404–427.
344 A. Shafeen, E. Croiset, P. L. Douglas and I. Chatzis, *Energy Convers. Manage.*, 2004, **45**, 3207–3217.
345 D. Singh, E. Croiset, P. L. Douglas and M. A. Douglas, *Energy Convers. Manage.*, 2003, **44**, 3073–3091.
346 E. Mohammad-Pajooh, D. Weichgrebe, G. Cuff, B. M. Tosarkani and K.-H. Rosenwinkel, *Chemosphere*, 2018, **212**, 898–914.
347 R. B. Jackson, A. Vengosh, J. W. Carey, R. J. Davies, T. H. Darrah, F. O'Sullivan and G. Pétron, *Annu. Rev. Environ. Resour.*, 2014, **39**, 327–362.
348 J. Zhou, G. Liu, Y. Jiang, X. Xian, Q. Liu, D. Zhang and J. Tan, *J. Nat. Gas Sci. Eng.*, 2016, **36**, 369–377.
349 H. Wang, G. Li, Y. Zheng, S. Kamy, Z. Shen, B. Yang and L. Shi, *Acta Pet. Sin.*, 2020, **41**, 116–126.
350 X. Lei, T. Tamagawa, K. Tezuka and M. Takahashi, *Geophys. Res. Lett.*, 2011, **38**, 1–5.
351 R. Wilkins, A. H. Menefee and A. F. Clarens, *Environ. Sci. Technol.*, 2016, **50**, 13134–13141.
352 D. J. Soeder, S. Sharma, N. Pekney, L. Hopkinson, R. Dilmore, B. Kutchko, B. Stewart, K. Carter, A. Hakala and R. Capo, *Int. J. Coal Geol.*, 2014, **126**, 4–19.
353 P. Noothout, F. Wiersma, O. Hurtado, D. Macdonald, J. Kemper and K. van Alphen, *Energy Procedia*, 2014, **63**, 2481–2492.
354 M. J. Kennedy, D. R. Pevear and R. J. Hill, *Science*, 2002, **295**, 657.
355 J. Liming, Q. Junli, Z. Tongwei and X. Yanqing, *Earth Sci.*, 2012, **37**, 1043–1050.
356 Z. T. Bieniawski, *Int. J. Rock Mech. Min. Sci. Geomech. Abstr.*, 1968, **5**, 325–335.
357 Q. Lyu, P. Ranjith, X. Long, Y. Kang and M. Huang, *Arabian J. Geosci.*, 2015, **8**, 10289–10299.
358 R. Lahann, M. Mastalerz, J. A. Rupp and A. Drobniak, *Int. J. Coal Geol.*, 2013, **108**, 2–9.
359 M. Mastalerz, A. Drobniak and J. Rupp, *Energy Fuels*, 2008, **22**, 4049–4061.
360 L.-P. Yi, X.-G. Li, Z.-Z. Yang and J. Sun, *Int. J. Heat Mass Transfer*, 2018, **121**, 680–690.
361 H. Wang, X. Li, K. Sepehrnoori, Y. Zheng and W. Yan, *Int. J. Heat Mass Transfer*, 2019, **139**, 10–16.
362 J. Wang, B. Sun, H. Li, X. Wang, Z. Wang and X. Sun, *Int. J. Heat Mass Transfer*, 2018, **118**, 1012–1021.
363 G. Linga and H. Lund, *Int. J. Greenhouse Gas Control*, 2016, **51**, 71–80.
364 B. Sun, J. Wang, Z. Wang, Y. Gao and J. Xu, *J. Pet. Sci. Eng.*, 2018, **166**, 420–432.
365 L. Hou, B. Sun, Z. Wang and Q. Li, *J. Supercrit. Fluids*, 2015, **100**, 121–128.
366 Z. Shuli, H. Zengping and P. Jiadong, *China Petroleum Machinery*, 2016, **44**, 79–84.